FINAL TECHNICAL REPORT

Synthetic, Structural and Mechanistic Investigations of Olefin Polymerization Catalyzed by Early Transition Metal Compounds

DOE-FG02-85ER13431

John E. Bercaw, Department of Chemistry, California Institute of Technology,
Pasadena, CA 91125
626-395-6577, bercaw@caltech.edu

Introduction

Our DOE support almost 30 years ago in support of our investigations of our mechanistic studies of olefin insertion/β-H elimination for the well behaved system, reversible rearrangements for olefin hydrides of the general formula $Cp'_2M(CH_2{=}CHR)H$ (M = Nb, Ta; Cp′ = (η^5-C_5H_5) , (η^5-C_5Me_5) (Scheme 1). In the case of the niobocene systems we observe approximately equal concentrations of syn and anti geometric isomers, whereas for steric reasons the syn isomer is much more stable for the permethylniobocene series of olefin hydrides (Scheme 2) . We probed the rate for olefin insertion (k_1) and established relative ground state energies from the equilibrium constants for olefin exchange (K_{eq}) for a series of such olefin hydride complexes, and thus mapped out the free energy profiles for complexes having variable electronic (R = para-C_6H_4X (X = CF_3, H, CH_3, OCH_3, and NMe_2) and steric (R = H, CH_3, C_6H_5) effects.

Scheme 1

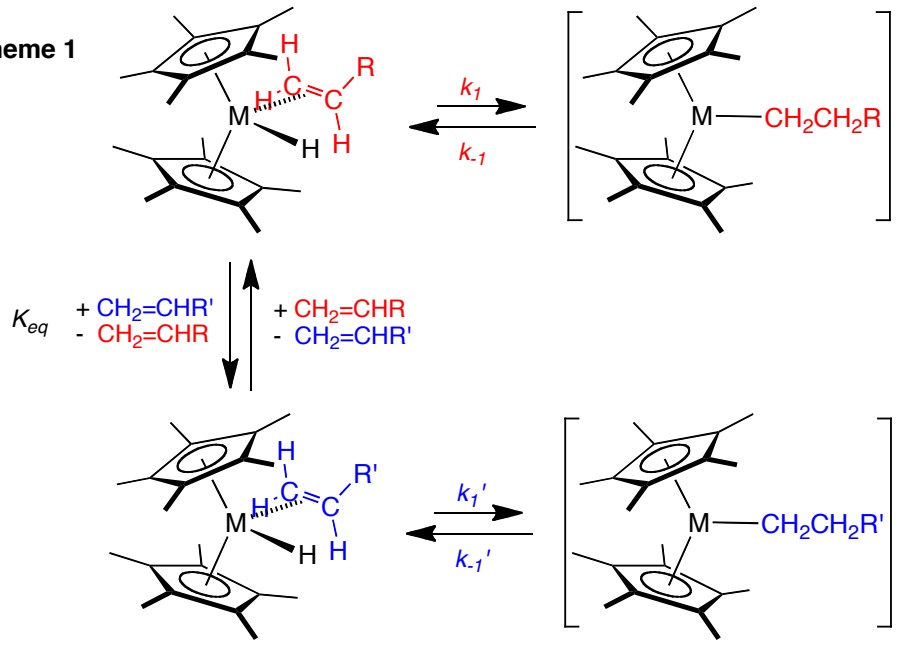

Scheme 2

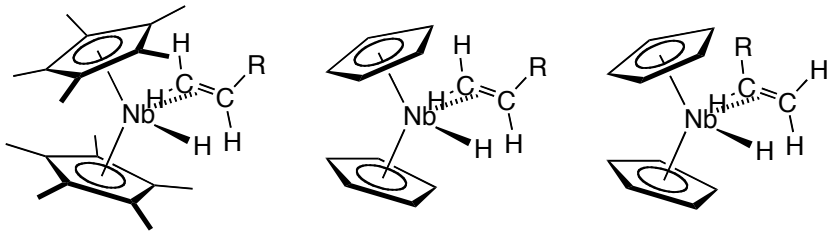

syn *syn* *anti*

A self consistent picture of the ground state and transition state preferences emerged from these studies (Scheme 3), with the following conclusions: (1) the ground state olefin hydride is favored electronically for R electron-withdrawing (olefin a better π acid), Cp = (η^5-C_5Me_5) and M = Ta (metal in higher oxidation state in ground state relative to product alkyl), and favored sterically for R small and Cp = (η^5-C_5H_5), and (2) the transition state for the endothermic formation of the alkyl product formed by olefin insertion is favored electronically for R electron releasing (H migrates approximately as hydride) and R' electron withdrawing (charge distribution in four center transition state alternates as shown).

Scheme 3

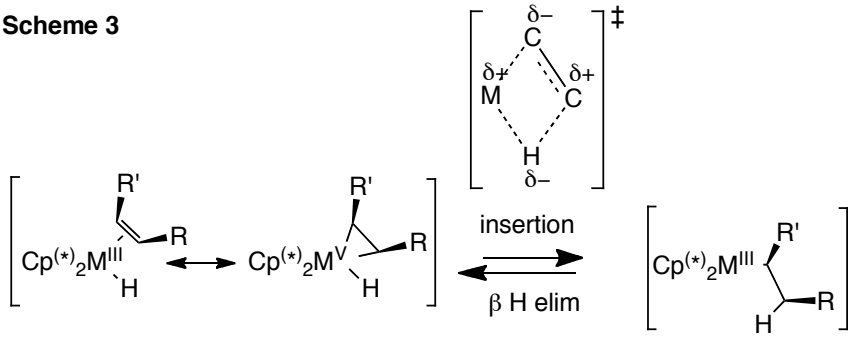

During the past few decades the application of early transition metal compounds to catalytic transformations has grown in scope and scale. The largest volume processes are in the production of polyolefins with worldwide production exceeding 100 billion pounds per year. Metallocene and other "single site" catalysts,[1] have transformed the polyolefin industry, particularly for ethylene/1-alkene copolymers as well as ethylene/propylene and ethylene/propylene/diene elastomers.[2] Whereas late transition metal catalysts based on iron, nickel, and palladium have been developed,[3,4] early transition metals, particularly titanium and zirconium, dominat commercially important catalysts.[5] Significant advancements have also been made using metallocene and non-metallocene early transition metal complexes to effect other catalytic transformations, *e. g.* catalytic additions of HX (X = SiR_3, AlR_2, BR_2, NR_2) to multiple carbon-carbon bonds.[6] These developments have been possible due to synthetic and mechanistic studies of fundamental transformations for new

organometallic compounds. Clever application by academic and industrial chemists of these steps to catalytic cycles has often followed. Remarkable reaction sequences have been recently reported: (a) hydro(aminoalkyl)ation,[7] or (b) conversions of short chain hydrocarbons to more valuable longer chain ones through highly selective ethylene tri- or tetramerization,[8] direct alkane metathesis, or a two-step dehydrogenation/metathesis type route,[9] This last example points to potentially very significant new direction for early transition metal catalysis: coupling well-established early transition metal catalytic process (such as olefin metathesis) with late transition metal catalysis (transfer dehydrogenation) to effect a net transformation that neither could do independently.

Summary of Progress During Most Recent Past Grant Periods

During most immediate past grant periods our group has been engaged in research aimed at establishing the mechanisms of fundamental steps occurring in olefin oligomerization and polymerization. Earlier work sought to define the underlying mechanisms of chain initiation, propagation and transfer, with special attention paid to issues of stereocontrol in α-olefin polymerization catalysis. Our early focus was on scandocene and yttrocene hydrides, alkyls and related compounds, well-behaved catalysts that allow studies of the kinetics and mechanism of ethylene propagation and chain transfer by β-H elimination. These neutral scandium and yttrium catalysts have allowed us to probe the nature of the transition states for olefin insertion with regard to the electronic influences of both the migrating group and the substituents at the β carbon atom of the growing polymer chain, without the complications of a possible role of the counter-anion. We have also obtained evidence for α-agostic assistance in the carbon-carbon bond-forming step for hydrocyclization of 1,5-hexadiene to methylcyclopentane and 1,6-heptadiene to methylcyclohexane, and for hydrodimerization of 1-hexene catalyzed by scandocene and yttrocene catalysts. As a result of our work and that of others, principally the Brintzinger group,[10] the bonding interactions operating in the transition state for chain propagation in propylene polymerizations have been established:

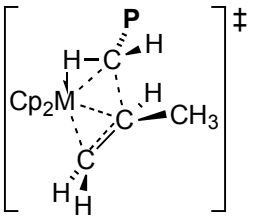

(**P** = polymer chain)

All metallocene catalysts have in common an active form that is a (possibly solvated) 14-electron configuration, hence a doubly coordinatively unsaturated metallocene alkyl (*i. e.*

M = $[Zr^{IV}]^+$, $[Hf^{IV}]^+$, Sc^{III}, Y^{III} or trivalent lanthanide) to allow for olefin coordination and α-agostic assistance in C-C bond formation. For isotactic polymerizations of propylene with chiral metallocene catalysts, it has been shown that stereoregularity is controlled primarily by the metallocene chirality and not by the asymmetry of the last inserted monomer unit. We have addressed the issues of stereocontrol, seeking to define the transition structures for isotactic, syndiotactic and hemi-isotactic polymerizations of α-olefins.

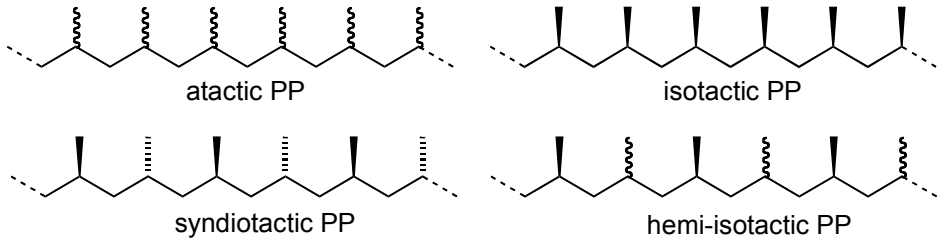

We initially chose to examine the simpler isotactic systems, since these operate by selecting the same enantioface of the α-olefin for each enchainment. Because both the absolute configuration for the metallocene catalyst and the enantiofacial preference for olefin insertion needed to be defined, we devised a new chiral ligand that may be prepared from enantiopure binaphthol, *e. g.* ({(η^5-C_5H_2-2-$SiMe_3$-4-CMe_3)$_2$Si(*R*-(+)-1,1'-bi-2-naphtholate)}, "*R*-BnBp", that coordinates to yttrium to afford a single enantiomerically pure *S*-yttrocene without forming the meso isomer or other enantiomer, *i. e.* this ligand self-resolves on metallation.[11] A chiral 1-pentene that allows the sense and extent of enantiofacial preference for addition to Y-H and Y-pentyl bonds to be determined by ^{1}H and ^{2}H NMR spectroscopy was designed and synthesized on multi-gram scales.[12]

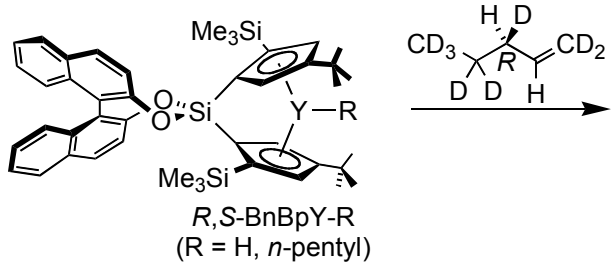

A model was developed to rationalize our findings, along with those from other laboratories: "chain segment control", where the chiral metallocene ligand array directs the C_α-C_β polymeryl segment in the α-agostic transition state, and the new C-C bond that is formed during monomer enchainment takes place with **P** and R in a trans geometry. A general consensus has been reached by the research community that this picture accounts for isoselective polymerizations with C_2-symmetric metallocene catalysts (Scheme 1).[3,13,14]

Scheme 1

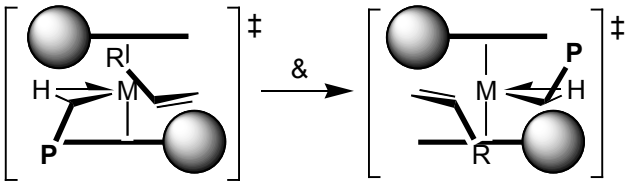

- C_2 symmetry relates two sides of metallocene wedge: they are homotopic
- two sides of metallocene wedge are identical, thus same enantioface of olefin is used for each enchainment, irrespective of side of wedge

We also designed and synthesized new doubly-[$SiMe_2$] linked ligand systems that afford highly active C_s-symmetric metallocene catalysts for α-olefin polymerization capable of polymerizing propylene with unprecedented syndiospecificities (as high as 99.4% [*r*], T_m = 151 °C; T_p = 20 °C, liquid propylene).[15]

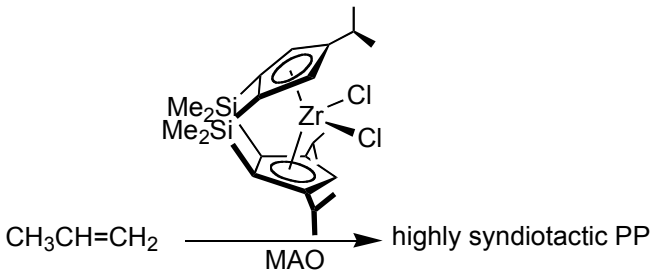

Investigations of the mechanisms of stereocontrol with this class of C_s-symmetric metallocene catalysts revealed the following key features: (1) the C_s-symmetric *ansa*-metallocene structure has one cyclopentadienyl possessing bulky substituents flanking the center of the metallocene wedge to direct the polymer chain segment (up) toward the less substituted cyclopentadienyl, whether it resides on the left or right side in the transition structure for propagation (Scheme 2), (2) an open region between the bulky substituents on the lower cyclopentadienyl to accommodate the α-olefin alkyl (methyl for propylene), which is directed by the polymer segment trans (down), the dominant steric interaction in the transition structure, and (3) migratory insertions that result in regular alternation of the monomer approach from the left and right side of the metallocene wedge.

Scheme 2

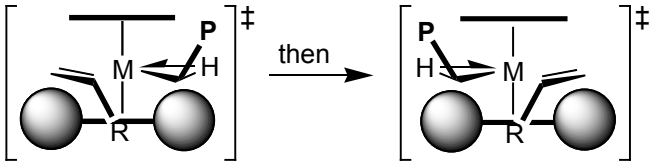

- C_s symmetry relates two sides of metallocene wedge: they are enantiotopic
- approach of olefin from alternating sides of metallocene wedge naturally results in regular alternation of enantiofaces in enchainments and a syndiotactic structure

By conducting polymerizations at varying temperatures and monomer concentrations, the principal stereoerror-producing process for these C_s-symmetric catalysts has been identified: following an enchainment, inversion at zirconium resulting in "site epimerization" (by polymeryl chain swinging) prior to monomer coordination.[16] The C_1-symmetric members of the class of doubly [$SiMe_2$]-linked zirconocene catalysts display an unusual dependence of stereospecificity on propylene concentration, switching from isospecific to syndiospecific with increasing propylene pressure, consistent with competitive unimolecular site epimerization process and a bimolecular chain propagation.

Other synthetic and structural studies related to polymerization by these catalysts were also reported earlier.[17,18,19,20,21,22,23, 24,25,26] More directly related to α-olefin polymerizations with metallocene catalysts: (*i*) A new strategy for producing elastomeric polypropylene with catalysts derived from $R'_2C(\eta^5\text{-}3\text{-}R\text{-}C_5H_3)(\eta^5\text{-}C_{13}H_8)MCl_2$/MAO (M = Zr, Hf; ($\eta^5$-$C_{13}H_8$) = fluorenyl; MAO = methylaluminoxane) was developed.[27,28] (*ii*) Aspects of ancillary ligand effects on olefin binding to cationic zirconocene alkyls were probed with a pendant olefin strategy.[29] (*iii*) Using a doubly labeled propylene monomer CH_2=$CD^{13}CH_3$, the mechanism of chain epimerization during propylene polymerization with C_2-symmetric zirconocene catalysts was probed. The mechanism suggested by Busico[30] was supported by our findings: racemization at the β-carbon of the polymeryl chain via tertiary alkyl complexes formed by reversible β-H elimination and olefin rotation. The absence of observable [-$CH_2CH^{13}CH_2D$-] in the [*mrrm*] pentad region of the ^{13}C NMR spectra provides evidence that an allyl/dihydrogen complex does *not* mediate chain epimerization.[31] (*iv*) distal ligand influences are found to have surprising and dramatic effects on polymer stereochemistry in propylene polymerization with metallocene catalysts.[32] Highly stereoregular syndiotactic polypropylene is obtained with the catalyst systems **1**/MAO (MAO = methylaluminoxane) and **2**/MAO.

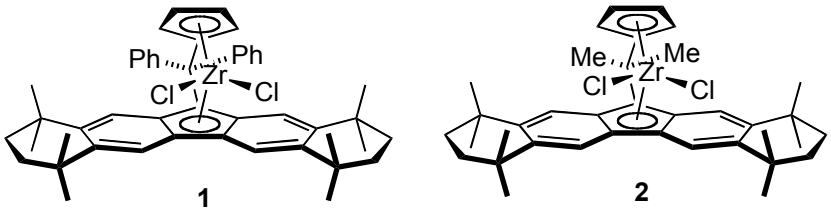

1 2

(*v*). ***Cyclopentadienyl and Olefin Substituent Effects on Insertion and β-Hydrogen Elimination with Group 4 Metallocenes. Kinetics, Mechanism and Thermodynamics for Zirconocene and Hafnocene Alkyl Hydride Derivatives.*** We have also reported on an investigation of cyclopentadienyl and olefin substituent effects on the rates and thermodynamics of olefin insertion and β-H elimination for group 4 metallocene systems.[33] With the expectation that we my ultimately be able to obtain a predictive correlation between cyclopentadienyl substitution pattern and polymer molecular weight, we have examined reactions of group 4 metallocene dihydrides, $(R_nCp)_2MH_2$ (R_nCp = alkyl substituted cyclopentadienyl; M = Zr, Hf), with olefins to afford stable metallocene alkyl-hydride complexes of the general formula, $(R_nCp)_2M(CH_2CHR'_2)(H)$ (R' = H, alkyl). For sterically crowded, monomeric dihydrides, second order rate constants for olefin insertion have been measured. Striking steric effects for olefin insertion and a primary k_H/k_D of 2.4(3) at 23 °C and a linear free energy correlation to σ (ρ = -0.46(1)) for para-substituted styrene insertion indicate that insertion into a Zr-H bond proceeds via rate determining hydride transfer to coordinated olefin (Scheme 3), with small positive charge buildup at the β carbon of the inserting styrene.

Scheme 3

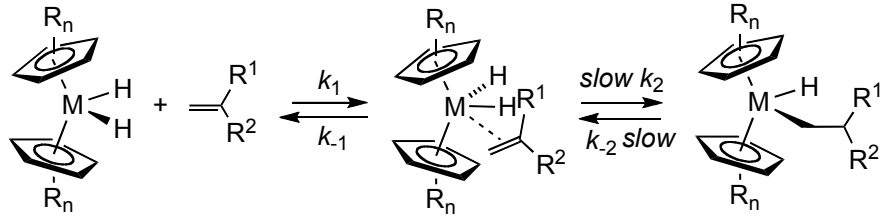

The rates of β-H elimination for the series $(R_nCp)_2Zr(CH_2CHR')(H)$ have been measured via rapid trapping of the intermediate zirconocene dihydride with 4,4-dimethyl-2-pentyne, and key features have been established: (a) primary kinetic deuterium isotope effect (k_H/k_D = 3.9 to 4.5) and (b) a linear free relationship for the phenethyl hydride series, $Cp^*(\eta^5\text{-}C_5Me_4H)Zr(CH_2CH_2\text{-}p\text{-}C_6H_4\text{-}X)(H)$ (X = H, CH_3, CF_3, OCH_3), that correlates better to σ than σ^+; ρ = -1.80(5). Equilibration of a series of $Cp^*(CpR_n)Zr(CH_2CHMe_2)(H)$ and $Cp^*(CpR_n)Zr(CH_2CH_2CH_2CH_3)(H)$ with free isobutene and 1-butene has established the relative ground state energies of isobutyl and *n*-butyl complexes, and, in combination with

the free energies of activation for β-H elimination, free energy profiles were constructed for insertion and β-H elimination for each olefin.

(*vi*). ***The Mechanism of Isotactic Polypropylene Formation with C_1-Symmetric Metallocene Catalysts.*** A new C_1-symmetric zirconocene catalyst $[Me_2C(3\text{-}tert\text{-butyl-}C_5H_3)(C_{13}H_8)]ZrCl_2$/MAO (MAO = methylaluminoxane, $C_{13}H_8$ = fluorenylidene) was prepared, and this precatalyst was shown to produce isotactic polypropylene. Evidence supports an alternating mechanism, where both sites of the metallocene wedge are utilized for monomer insertion (blue pathway of Scheme 4), rather than the previously proposed site epimerization (inversion at Zr) following each monomer insertion. As the polymerization temperature increases (0 to 60 °C) with lower concentrations of propylene, the site epimerization mechanism (red pathway of Scheme 4) begins to compete, as evidenced by an increase in isotacticity. The alternating mechanism also accounts for polypropylene microstructures obtained with $Me_2C(3\text{-R-}C_5H_3)(Oct)ZrCl_2$/MAO, where Oct = octamethyloctahydrodibenzofluorenylidene and R = methyl, cyclohexyl, diphenylmethyl, and with $Me_2C(3\text{-}tert\text{-butyl-4-Me-}C_5H_2)(Oct)ZrCl_2$/MAO. For an Oct-containing catalyst system with R = 2-methyl-2-adamantyl, unprecedentedly high (for a fluorenyl-based metallocene catalyst) isotacticity ([*mmmm*] > 99%) is obtained; the polymer prepared at 0 °C has T_m = 167 °C and M_w = 370 000.

Scheme 4

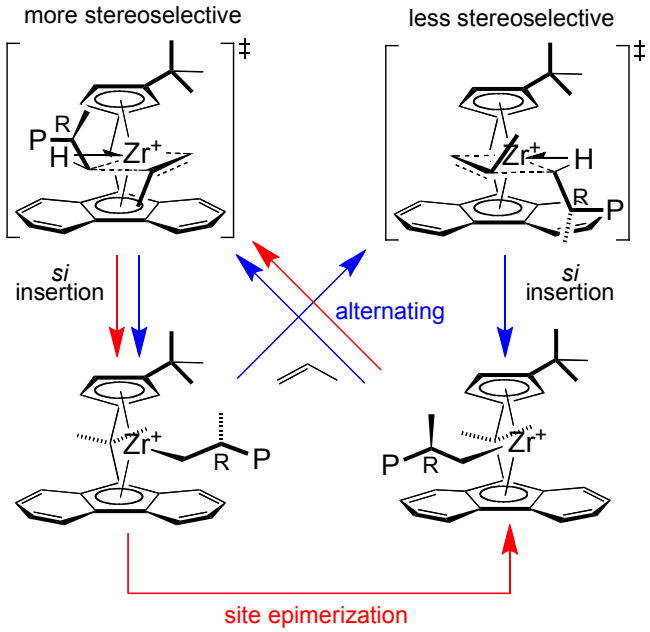

(*vii*). ***Nitrogen-Linked Diphosphine Ligands with Ethers Attached to Nitrogen for Chromium Catalyzed Ethylene Tri- and Tetramerizations.*** A series of *bis*(diphenylphosphino)amine ligands with a donor group attached to the nitrogen linker, when metallated with chromium trichloride, provides precursors to highly active, relatively stable, and selective precatalysts for trimerization and tetramerization of ethylene.[34] Precatalyst **8**, when activated with MAO, is particularly active. It has been demonstrated in oligomerization reactions performed at 1 and 4 atm of ethylene that these new systems increase total productivity by enhancing catalyst stability, as compared with those lacking a donor group on the diphosphine ligand, presumably by weak coordination of the ether oxygen to a coordinatively unsaturated chromium species. Furthermore, the use of chlorobenzene solvent (rather than toluene) significantly improves productivity, stability and selectivity. The product distributions and minor byproducts provide information relevant to mechanistic issues surrounding these types of reactions.

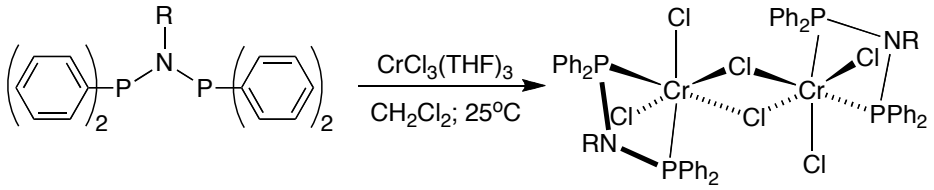

6: R = $(CH_2)_2OCH_3$
7: R = $(CH_2)_3OCH_3$
8: R = $(o\text{-}OCH_3)C_6H_4$
9: R = $CH_2(o\text{-}OCH_3)C_6H_4$

Close examination of the C_6 side-products formed in these trimerization/tetramerization reactions revealed that the two main side-products within the C_6 fraction are methylcyclopentane and methylenecyclopentane. Both of these products suggest the hexenyl-hydride (or octenyl-hydride) mediated pathway(s), perhaps operating in parallel with concerted 3,7 (or 3,9) hydride shift(s) from a chromacycloheptane (or chromacyclononane) intermediate(s) that lead to 1-hexene and 1-octene. Formation of methylcyclopentane may be readily accommodated by olefin re-insertion into the Cr-C bond followed by C-H reductive elimination; methylenecyclopentane by the possible routes shown (Scheme 5).

Scheme 5

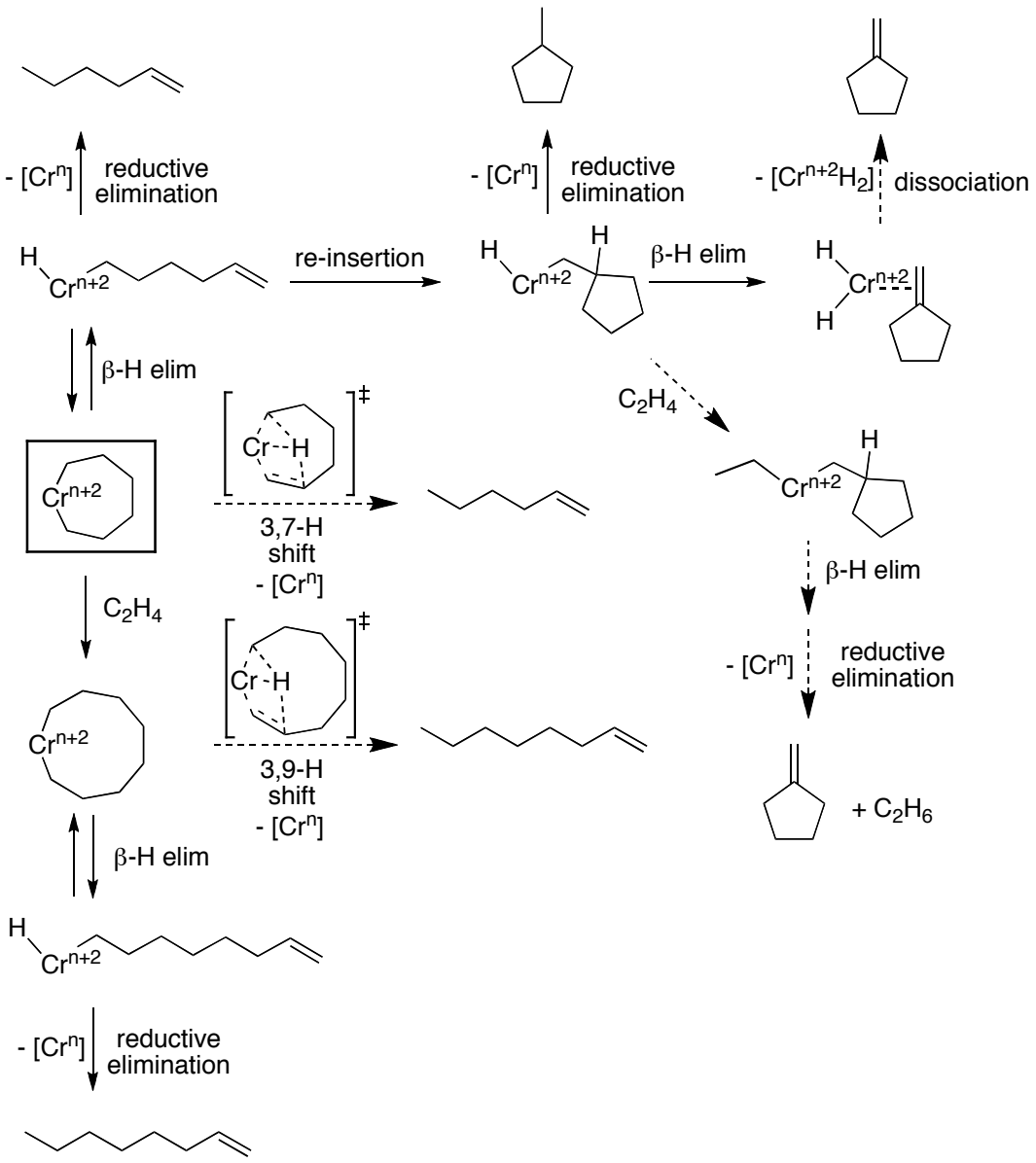

(*viii*). ***Mechanistic Studies of Olefin and Alkyne Trimerization with Chromium Catalysts – Deuterium Labeling and Studies of Regiochemistry Using a Model Chromacyclopentane Complex.*** Mechanistic studies have addressed the elementary steps involved in ethylene trimerization catalyzed by these "PNP"-ligated chromium complexes.[35] Thus, the mechanism of olefin trimerization reaction utilizing chromium(III) precursors supported by diphosphine ligand PNP^{O4} = $(o\text{-}MeO\text{-}C_6H_4)_2PN(Me)P(o\text{-}MeO\text{-}C_6H_4)_2$was examined using deuterium labeling and studies of reactions with α-olefins and internal olefins. A well defined chromium precursor utilized in this studies is $Cr(PNP^{O4})$(o,o'-biphenyldiyl)Br (**9**).

Scheme 6

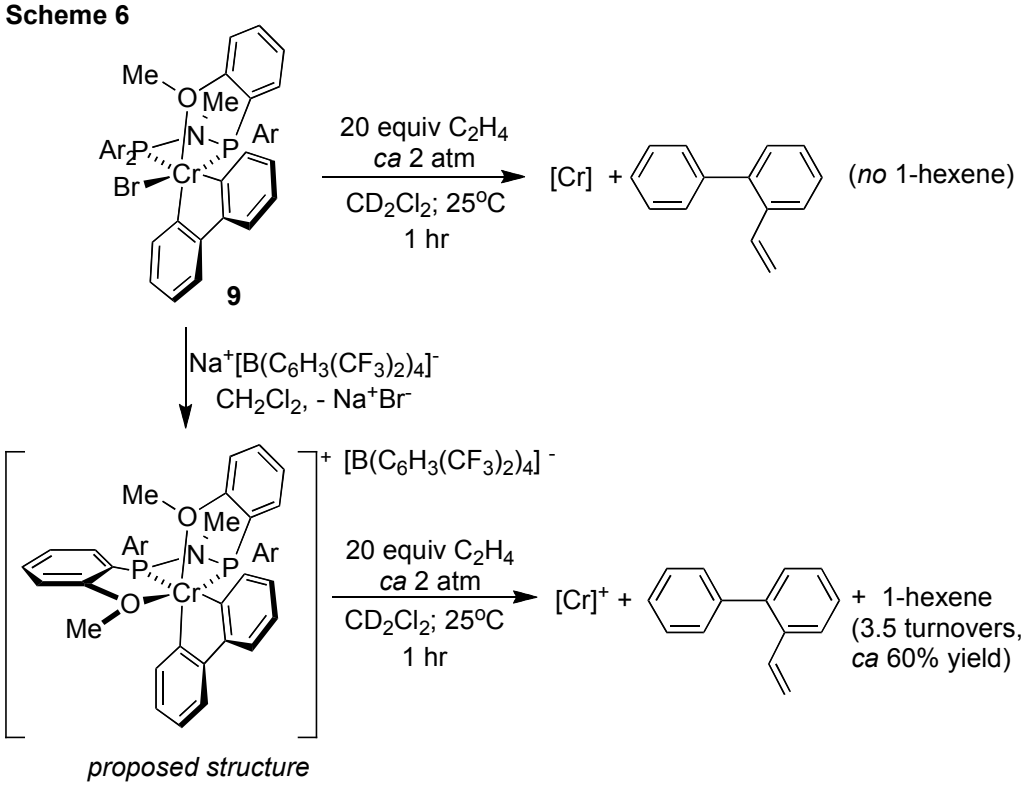

A cationic species, obtained by halide abstraction with $NaB[C_6H_3(CF_3)_2]_4$, is required for catalytic turnover to generate 1-hexene from ethylene. The initiation byproduct is vinylbiphenyl; this is formed even without activation by halide abstraction. Trimerization of 2-butyne is accomplished by the same cationic system but not by the neutral species. Catalytic trimerization, with various [(PNP^{O4})Cr] precursors, of a 1:1 mixture of C_2D_4 and C_2H_4 gives isotopologs of 1-hexene without H/D scrambling (C_6D_{12}, $C_6D_8H_4$, $C_6D_4H_8$, and C_6H_{12} in a 1:3:3:1 ratio). The lack of crossover supports a mechanism involving metallacyclic intermediates. Using a SHOP catalyst to perform the oligomerization of a 1:1 mixture of C_2D_4 and C_2H_4 leads to the generation of a broader distribution of 1-hexene isotopologs, consistent with a Cossee-type mechanism for 1-hexene formation. The ethylene trimerization reaction was further studied by the reaction of trans-, cis-, and gem-ethylene-d_2 upon activation of Cr(PNP^{O4})(o,o'-biphenyldiyl)Br with $NaB[C_6H_3(CF_3)_2]_4$. The trimerization of cis and trans ethylene-d_2 generates 1-hexene isotopomers having differing terminal CDH groups, with an isotope effect of 3.1(1) and 4.1(1), respectively. These results are consistent with reductive elimination of 1-hexene from a putative {Cr(PNP^{O4})(H)[$(CH_2)_4CH{=}CH_2$]} occurring much faster than a hydride 2,1-insertion or with concerted 1-hexene formation from a chromacycloheptane via a 3,7-H shift. The trimerization of gem-ethylene-d_2 has an isotope effect of 1.3(1), consistent with irreversible formation of a chromacycloheptane intermediate on route to 1-hexene formation. Reactions of olefins with a model chromacyclopentane was investigated starting from Cr(PNP^{O4})(o,o'-biphenyldiyl)Br.

α-Olefins react with cationic biphenyldiyl chromium species **9** to generate products from 1,2-insertion. A study of the reaction of 2-butenes indicated that β-H elimination occurs preferentially from the ring CH rather than *exo*-CH bond in the metallacycloheptane intermediates. A study of cotrimerization of ethylene with propylene correlates with these findings of regioselectivity. Competition experiments with mixtures of two olefins indicate that the relative insertion rates generally decrease with increasing size of the olefins.

(*ix*)**.** ***Kinetic Resolution of Chiral Olefins by Polymerization.*** As regards to our project aimed at developing olefin polymerization catalysts for kinetic resolution of chiral olefins, we have examined (a) whether catalyst site epimerization during the polymerization erodes the enantioselectivity, and (b) the degree of monomer antipode selection by enantiomorphic site *vs* chain end control mechanisms.

(a) ***Catalyst Site Epimerization during the Kinetic Resolution of Chrial α Olefins by Polymerization***. A new enantiopure C_1-symmetric olefin polymerization precatalyst, (1,2-$SiMe_2$)$_2${η^5-C_5H_2-4-((*S*)-CHEtCMe$_3$)}{η^5-C_5H-3,5-($CHMe_2$)$_2$}$ZrCl_2$, **(*S*)-4b**, was synthesized, and its use for the kinetic resolution of 3-methyl-substituted racemic α-olefins was investigated.[36] Upon activation with methyl aluminoxane (MAO), selectivity factors for most olefins were greater when **(*S*)-4b** was used as the catalyst as compared to its previously reported methylneopentyl analog, (1,2-$SiMe_2$)$_2${η^5-C_5H_2-4-((*S*)-CHMeCCMe$_3$)}{η^5-C_5H-3,5-($CHMe_2$)$_2$}$ZrCl_2$, **(*S*)-4a**.

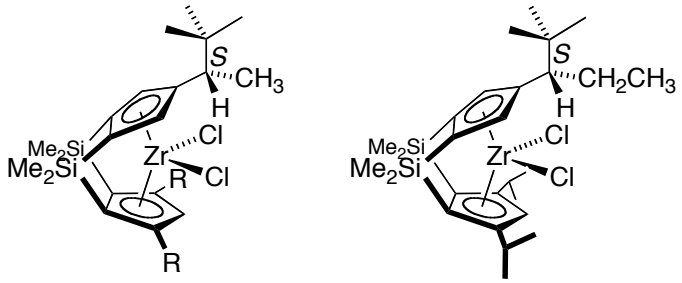

(R = *i*-Pr (***S*)-4a**, 3-pentyl, cyclohexyl) (***S*)-4b**

Pentad analysis of polypropylene produced by the two catalysts at various propylene concentrations indicates that **(*S*)-4b** undergoes more efficient site epimerization (polymeryl chain swinging prior to subsequent monomer enchainment) at intermediate propylene concentrations compared to **(*S*)-4a** (Scheme 7).

Scheme 7

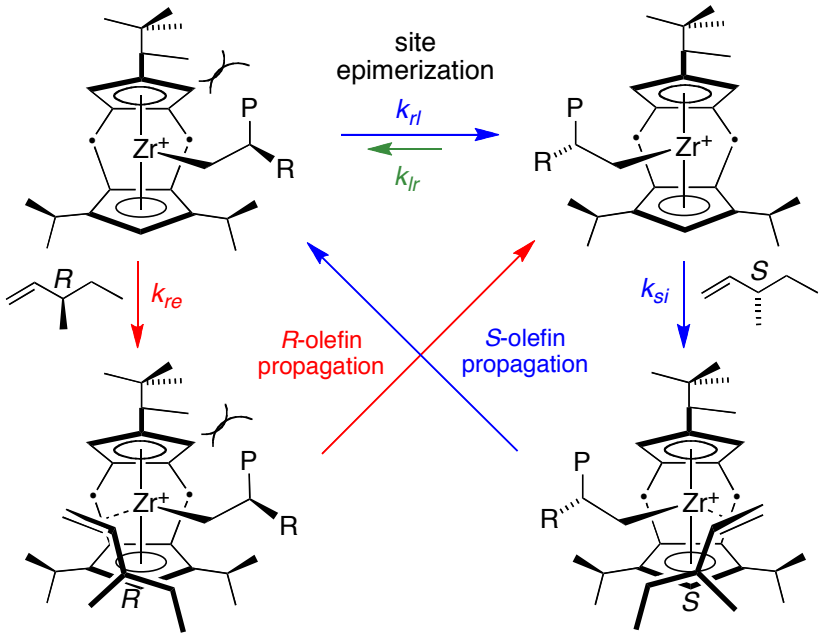

(P = remaining polymer chain; R = $CH(CH_3)CH_2CH_3$)

- blue pathway much faster than red pathway with relatively fast site epimerization yields isotactic polymer and (*S*) olefin enchainments
- alternating (red, then blue, then red, *etc.*) pathway with relatively slow site epimerization yields syndiotactic polymer and (*R*) and (*S*) olefin enchainments

At high and low propylene concentrations, however, the two catalysts behave similarly. On the other hand, polymerization of 3,5,5-trimethyl-1-hexene at different olefin concentrations and temperatures illustrated that selectivity differences between the two catalysts are likely not a consequence of inefficient site epimerization for **(*S*)-4b**.

(b) ***Kinetic Resolution of Racemic α-Olefins with Ansa-Zirconocene Polymerization Catalysts: Enantiomorphic Site vs. Chain End Control.*** Copolymerization of racemic 3-methyl-substituted α-olefins with ethylene and propylene were carried out in the presence of enantiopure C_1-symmetric *ansa* metallocene, {1,2-$(SiMe_2)_2$(η^5-3,5-$C_5H_1(CHMe_2)_2$)(η^5-4-C_5H_2((*S*)-$CHMeCMe_3$)]}$ZrCl_2$ ((*S*-**4**) to probe the affect of the polymer chain end on enantioselection for the *R*- or *S*-α-olefin during the kinetic resolution by polymerization catalysis.[37] The strategy involves "running out" the chiral chain end arising from a chiral monomer enchainment by several enchainments of achiral monomer prior to a subsequent insertion of chiral monomer, thus removing stereocontrol at the chiral branch of the β-carbon between successive chiral monomer enchaiments (Scheme 8).

Scheme 8

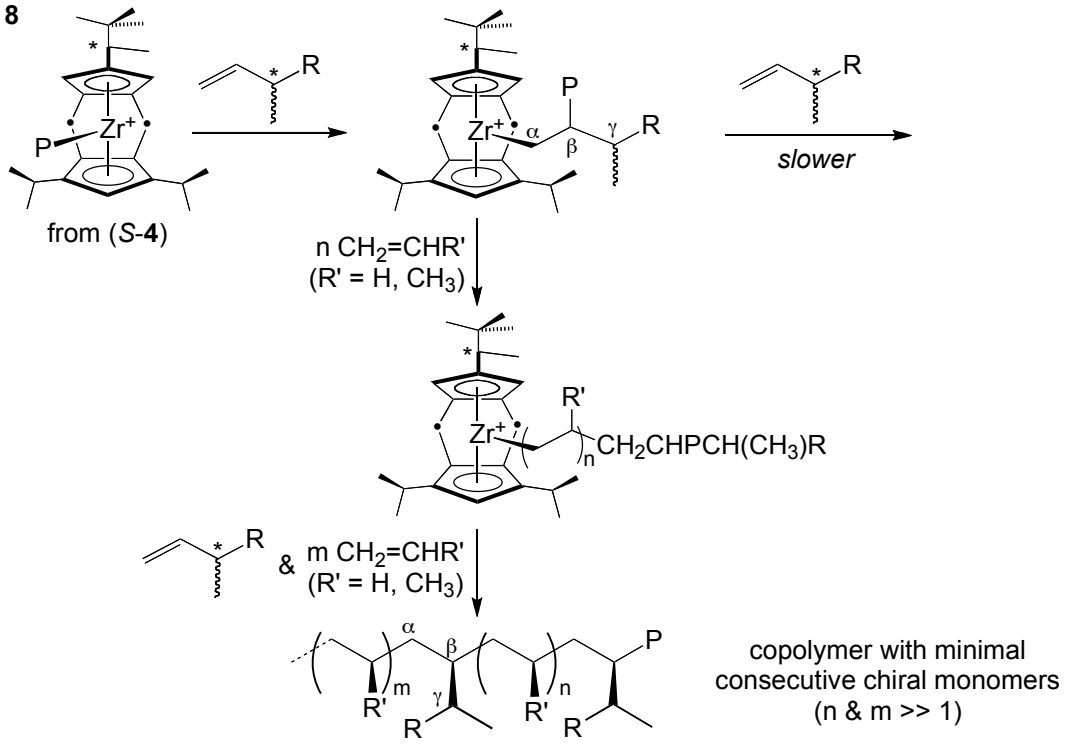

Copolymerizations with ethylene typically display a preference for enchainment of the *S* chiral monomer (as do homopolymerizations), with somewhat lower selectivities than for homopolymerizations, suggesting that the polymer chain end is an important factor in the enantioselection of the reaction, and that for homopolymerization, chain end control generally works cooperatively with enantiomorphic site control. For 3,4-dimethyl-1-pentene or 3,4,4-trimethyl-1-pentene, copolymerization with propylene yields much lower selectivities than either homopolymerization or copolymerization with ethylene, suggesting that chain end control arising from a methyl group at the β carbon along the main chain works uncooperatively with enantiomorphic site control, while chain end control originating from the polymer side chain (β and γ chain end control) cooperate with site control for tacticity (Scheme 9).

Scheme 9

• ethylene/chiral comonomer copolymerization:
s determined by Zr* (enantiomorphic site control)

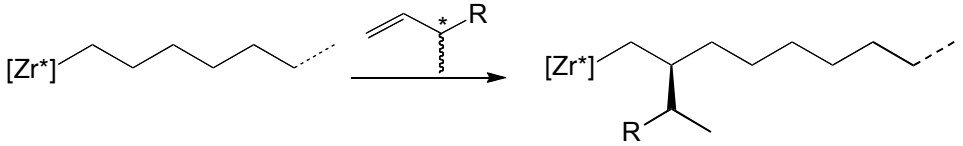

• propylene/chiral comonomer copolymerization:
s determined by Zr* and β_{C3} or β_{C3}' (site and β_{C3} chain end control)

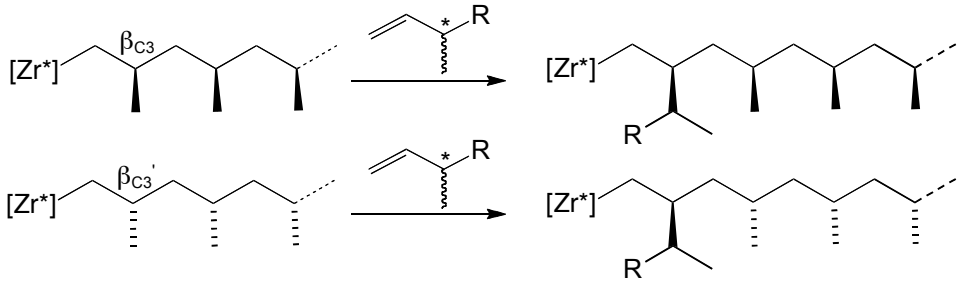

• homopolymerization of chiral monomer:
s determined by Zr*, β_{CM} and γ (site and β_{CM} and γ chain end control)

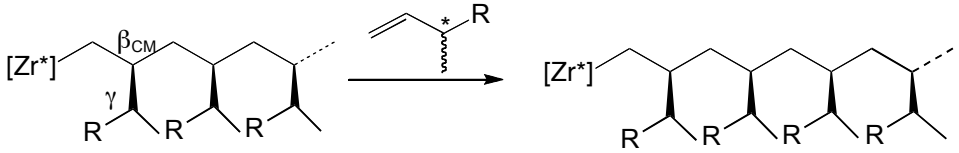

Whereas our data illustrate the complexity of the interplay of the various stereocontrol elements operating in these kinetic resolutions of chiral 3-methyl-1-alkenes using catalyst system **4**/MAO, we can draw the following conclusions:

(1) Enantiomorphic site control (Zr*) chooses for the same antipode with roughly the same stereoselection (*s*), in ethylene/chiral monomer copolymerizations as does the combination of Zr*, β_{CM}, and γ chain end control, implicating enantiomorphic site control as an important stereocontrol element.

(2) With the exception of 3-methyl-1-pentene, enantiomorphic site control and the β_{CM} and γ chain end control elements select for the same antipode of chiral monomer in the homopolymerizations, and hence the *s* values are larger for homopolymerizations than for ethylene/chiral monomer copolymerizations.

(3) For copolymerizations with propylene, where Zr* and chain end control arising from a β methyl group combine, surprisingly large offsetting effects on *s* are found for the alkenes having the sterically most demanding 3-substituents. The addition of β_{CM} and γ to Zr* more than restores the stereoselection lost by the combination of β_{C3} and/or β_{C3}' with Zr* for these two olefins.

(4) Whereas successful kinetic resolution ($s > 10$) is observed with 3,4-dimethyl-1-pentene, there are no clear correlations between the structure of the chiral olefin and the value of *s*, so that the guiding principles for design of a practical and general C_1-symmetric catalyst for

kinetic resolutions by polymerization of chiral monomers are not yet apparent. A successful and *general* strategy for kinetic resolution of chiral α-olefins will likely require a much larger enantiomorphic site control than that exhibited by (*S*)-**4**. Thus, this project has been, at least temporarily, put on hold.

(*x*). ***Group 3 Dialkyl Complexes with Tetradentate (L, L, N, O; L = N, O, S) Monoanionic Ligands.*** A new class of group 3 dialkyl complexes with tetradentate (L, L, N, O; L = N, O, S), monoanionic ligands has been developed, and the performance of olefin polymerization precatalysts has been examined.[38] Tripodal, tetradentate phenols, **10**, **11**, **12**, **13**, **14**, were synthesized, and metallations were performed *via* alkane elimination from yttrium and scandium *tris*-alkyl complexes to generate the corresponding dialkyl complexes **15a**, **15b**, **16a**, **16b**, **17**, and **18**.

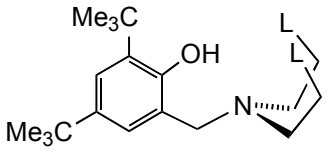

10: L = OCH_3
11: L = NEt_2

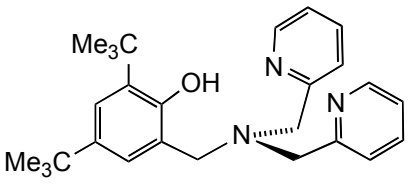

12

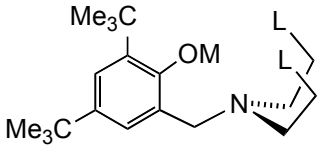

13: L = $SCMe_3$, M = Na
14: L = NMe_2, M = Li

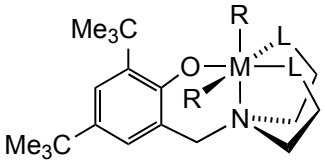

R = CH_2SiMe_2Ph
M = Y; L = OCH_3 (**15a**), NEt_2 (**15b**)
M = Sc; L = OCH_3 (**16a**), $SCMe_3$ (**16b**)

R = CH_2SiMe_3
M = Y; L = OCH_3 (**17**)
M = Sc; L = OCH_3 (**18**)

X-ray crystallographic studies show that **15a**, **15b**, and **16a** adopt, in the solid state, mononuclear structures of C_1 symmetry. The ^{1}H NMR spectra of these dialkyl complexes in benzene-d_6 at high temperatures reveal exchange processes involving the ether groups and the alkyl groups. The dynamic behavior of species **15a**, **16a** and **18** in toluene-d_8 was investigated by variable-temperature ^{1}H NMR spectroscopy. The activation parameters of the fluxional processes for **15a**, **16a** and **18** were determined by line-shape and Eyring analyses (for **15a**: $\Delta H^{\ddagger} = 7.3 \pm 0.3$ kcal/mol; $\Delta S^{\ddagger} = -16 \pm 1.4$ cal/mol·K; for **17a**: $\Delta H^{\ddagger} = 9.9 \pm 0.5$ kcal/mol; $\Delta S^{\ddagger} = -15.3 \pm 1.8$ cal/mol·K; for **18**: $\Delta H^{\ddagger} = 10.8 \pm 0.6$ kcal/mol; $\Delta S^{\ddagger} = -11.4 \pm 1.9$ cal/mol·K). These data establish that the dialkyl complexes **15a**, **16a** and **18** undergo a non-dissociative exchange process, and we propose a trigonal twist process proceeding through trigonal prismatic intermediates (Scheme 10).

Scheme 10

Pathway 1 inteconverts R_1 & R_2; L_1 & L_2.

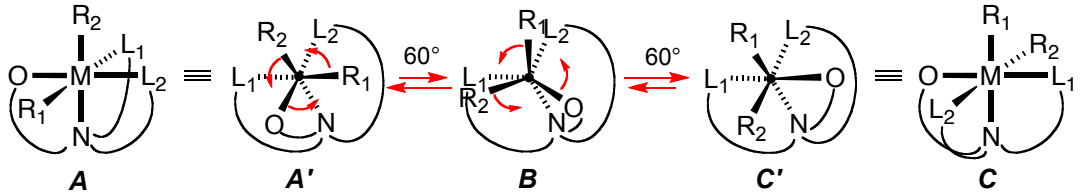

Pathway 2 interconverts L_1 & L_2; diastereotopic C*H*$_2$'s and Si(C*H*$_3$)$_2$Ph via C_s-symmetric isomer ***E***.

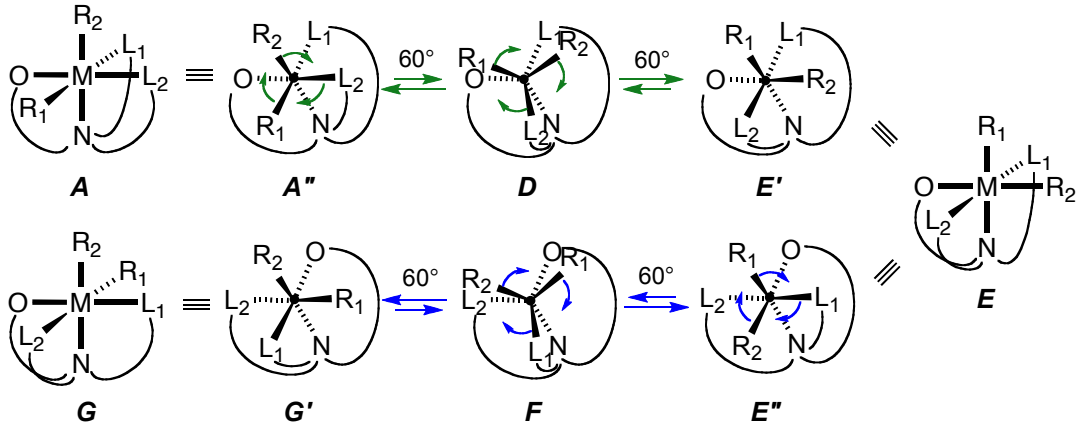

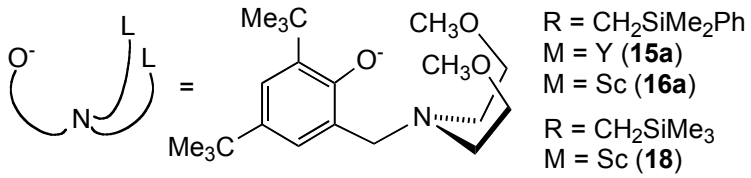

R = CH_2SiMe_2Ph
M = Y (**15a**)
M = Sc (**16a**)

R = CH_2SiMe_3
M = Sc (**18**)

The scandium dialkyl complex $[(C_5H_4N\text{-}2\text{-}CH_2)_2NCH_2\text{-}C_6H_2\text{-}3,5\text{-}(CMe_3)_2\text{-}2\text{-}O]Sc(CH_2SiMe_2Ph)_2$ (**19**) was found to undergo activation of a C-H bond of a methylene linking a pyridine to the central nitrogen donor, yielding one equivalent of $SiMe_3Ph$ and a "tuck-in" scandium product, following first order kinetics (k = 2.8(3) x 10^{-4} s^{-1} at 0 °C). These compounds were found to display disappointingly low polymerization activities. The yttrium dialkyl complexes **15a** and **16a** react with one equivalent of $[PhNHMe_2]^+[B(C_6F_5)_4]^-$ in chlorobenzene-d_5, to generate a solution that slowly polymerizes ethylene. Compounds **15 – 18** also polymerize ethylene with low activity upon activation with MAO.

(*xi*). ***Ti, Zr, and Hf Complexes Supported by Tridentate LX_2 Ligands having Two Phenolates Linked to Furan, Thiophene, and Pyridine Donors: Precatalysts for Propylene Polymerization and Oligomerization.*** The organometallic chemistry of early transition metals has, to a large extent, been advanced by the use of bent metallocene frameworks. The very strong ligand field imparted by the σ and π donor interactions of cyclopentadienyl ligands dominates the electronic structure, relegating the remaining three, nearly

non-bonding frontier orbitals to the "equatorial plane" in the wedge of the bent sandwich moiety. The (up to three) remaining ligand groups (*e.g.* H, alkyl, olefin, CO, PR_3, agostic C-H donors, *etc.*) that bind to the bent metallocene unit use these three frontier orbitals, and the metal-cyclopentadienyl bonding is relatively unaffected.

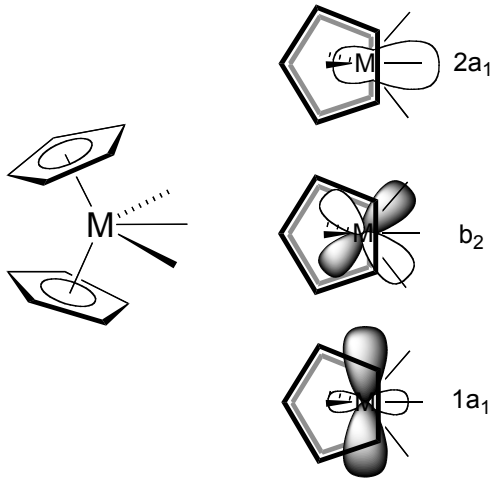

More recently there has been increased interest in using well defined, mono- and polydentate "non-metallocene" ligand sets to support a diverse range organometallic complexes of early transition metals, and fundamental transformations, catalysis, and small molecule activation have been investigated. Non-metallocene ligand sets offer a wide variety of symmetries and donor groups; these characteristics are particularly desirable for developing catalysts capable of effecting new stereocontrolled reactions.[39]

We have undertaken a major project to explore synthetic routes to semi-rigid, nonmetallocene catalysts for olefin polymerization and other transformations. Recognizing that *ansa*-metallocenes have provided the most important framework for single-site catalysts for α-olefin polymerization with tacticity control,[2acd] we have developed a semi-rigid ligand, LX_2-type pincer ligand family that has some of the same advantageous features of *ansa*-metallocenes. Titanium, zirconium, hafnium, vanadium, and tantalum complexes have been prepared thus far, and we have explored some of the features of their conformational preferences and the relative energies and spatial extensions of the frontier orbitals of the $[(LX_2)ML'_n]$ (n = 2, 3) moiety. Zirconium and titanium complexes with tridentate bis(phenolate)-donor (donor = pyridine, furan and thiophene) ligands have been prepared and investigated for applications in propylene polymerization.[40]

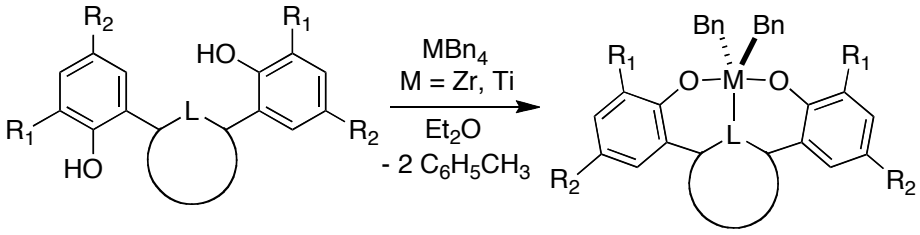

$R_1 = R_2 = CMe_3$, linker = pyridine
$R_1 = CEt_3$, R_2 = Me, linker = pyridine
$R_1 = R_2 = CMe_3$, linker = furan
$R_1 = R_2 = CMe_3$, linker = thiophene

The ligand framework has two "X-type" phenolates connected to the flat heterocyclic "L-type" donor at the 2,6- or 2,5- positions via direct ring-ring (sp^2-sp^2) linkages, and thus the geometry is more rigid than other variants that have sp^3 carbon linking moieties.[41,42] Bis(benzyl)titanium complexes with bis(phenolate)pyridine and -furan ligands and bis(benzyl)zirconium complexes with bis(phenolate)pyridine and -thiophene ligands have solid-state structures for the 5-coordinate titanium complexes that are roughly C_2-symmetric, while the 6-coordinate zirconium derivatives display C_s symmetry. The bis(phenolate)pyridine titanium complexes are structurally affected by the size of the substituents (CMe_3 or CEt_3) *ortho* to the oxygens – the larger group leading to a larger C_2 distortion from flat C_{2v}. Both titanium and zirconium dibenzyl complexes were found to be catalyst precursors for the polymerization of propylene upon activation with methylaluminoxane (MAO). The activities observed for the zirconium complexes are particularly notable, exceeding 10^6 g polypropylene/mol Zr·h in some cases. The bis(phenolate)pyridine titanium analogs are about 10^3 times less active, but generate polymers of higher molecular weight. When activated with MAO the titanium bis(phenolate)furan and bis(phenolate)thiophene systems were found to promote propylene oligomerization.

New sterically encumbered variants of the bis(phenolate) ligands were synthesized with pyridine linkers and benzene-diyl linkers and metallated with group 4 and 5 metal precursors to give complexes **20** – **26**. When activated with MAO these precatalysts polymerize ethylene and propylene and copolymerize ethylene and 1-hexene. The highest activity for propylene polymerization is observed with the vanadium precatalyst **21**: 8×10^5 g polypropylene/mol V·h, $M_w = 1.1 \times 10^6$, PDI = 2.03. Pre-catalysts **27** and **28** produce low molecular weight ($M_w \sim 10^4$) aPP with moderate activities (~5×10^4 g polypropylene/mol Ti·h). Pre-catalysts **20**, **22**, **23**, and **24** give mixtures of high molecular weight iPP and low molecular weight aPP, and with relatively low-to-moderate activies (~10^4 to 2×10^5 g polypropylene/mol metal·h). Pre-catalyst **25** gives only iPP via enantiomorphic site control, but with very low activity (~10^3 g polypropylene/mol Hf·h).

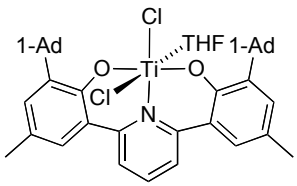

20

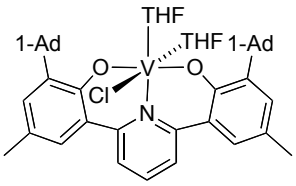

21

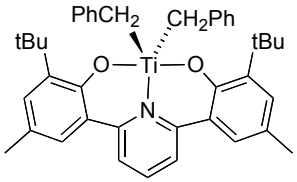

22

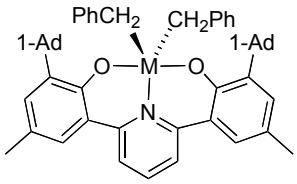

23, M = Ti
24, M = Zr
25, M = Hf

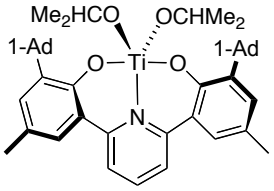

26

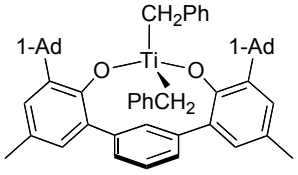

27

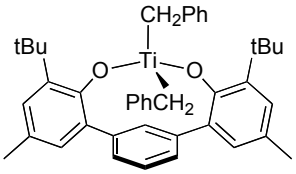

28

The solid state structures for **26**, **24-THF**, and **28** were determined. C_2 symmetry is found for **26**, with phenolate rings twisted (approximately 36° dihedral angle). On the other hand, **24-Et$_2$O** adopts a C_s-symmetric arrangement, and while C_s-symmetry is found for **28**, it displays a distorted tetrahedral geometry. In solution at room temperature, all of the bis(phenolate)pyridine-ligated precatalysts exhibit C_{2v}-averaged symmetries (^{1}H NMR)

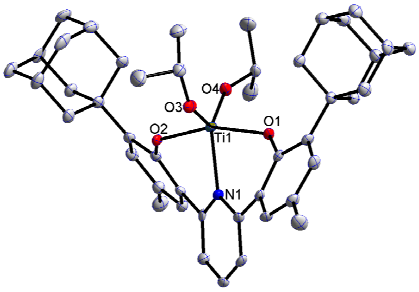

26

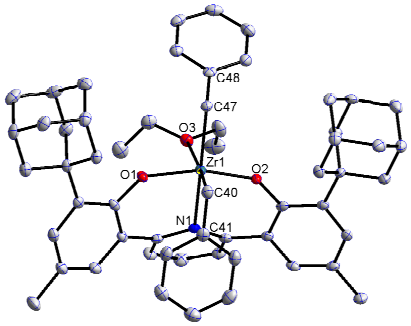

24-THF

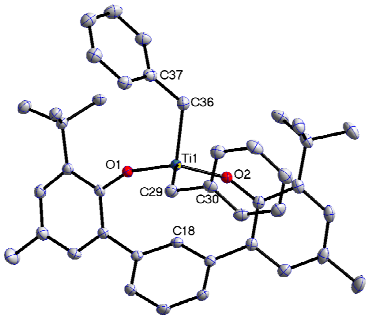

28

At this stage of the project, we concluded that the preferred conformations of the bis(phenolate) moiety of the ligand are rather unpredictable. Moreover, there appeared to be little correlation of polypropylene tacticity with solid state conformation of the precatalyst. Nor is it clear why the pyridine-linked bis(phenolate) complexes produce iPP and aPP with a bimodal molecular weight distribution; two catalytically active species are apparently generated when these precatalysts are activated with MAO. We have carried out some control experiments that rule out an bis(phenolate)pyridine-aluminum alkyl, generated by transmetallation of the ligand with either $AlMe_3$ or MAO, is catalytically active. We further considered the possibility that MAO complexes the nitrogen of a pyridine dissociated, for example, from the catalyst derived from **21** or **23**. The moderate activity of the catalysts derived from precatalyst **27** and **28**, and the atactic microstructure of the PP produced could be in support of this hypothesis. Thus, it is clear that these "first generation" LX_2 pincer

ligands may afford catalysts with high polymerization activities, but not with predictable tacticities.

(*xii*) ***Cyclometallated Tantalum Diphenolate Pincer Complexes.*** We have also examined the synthesis and reactivity of tantalum complexes supported by bidentate X_2 and tridentate LX_2 ligands having two phenolates linked to pyridine, thiophene, furan, and benzene connectors.[43] Using either alkane elimination or salt metathesis methods tantalum complexes have been prepared with new ligand systems having tridentate bis(phenolate)donor (donor = pyridine, furan, and thiophene) or bidentate bis(phenolate)benzene arrangements. The ligand framework has two "X-type" phenolates connected to the flat heterocyclic "L-type" donor at the 2,6- or 2,5- positions or to the 2,6-positions of benzene via direct ring-ring (sp^2-sp^2) linkages.

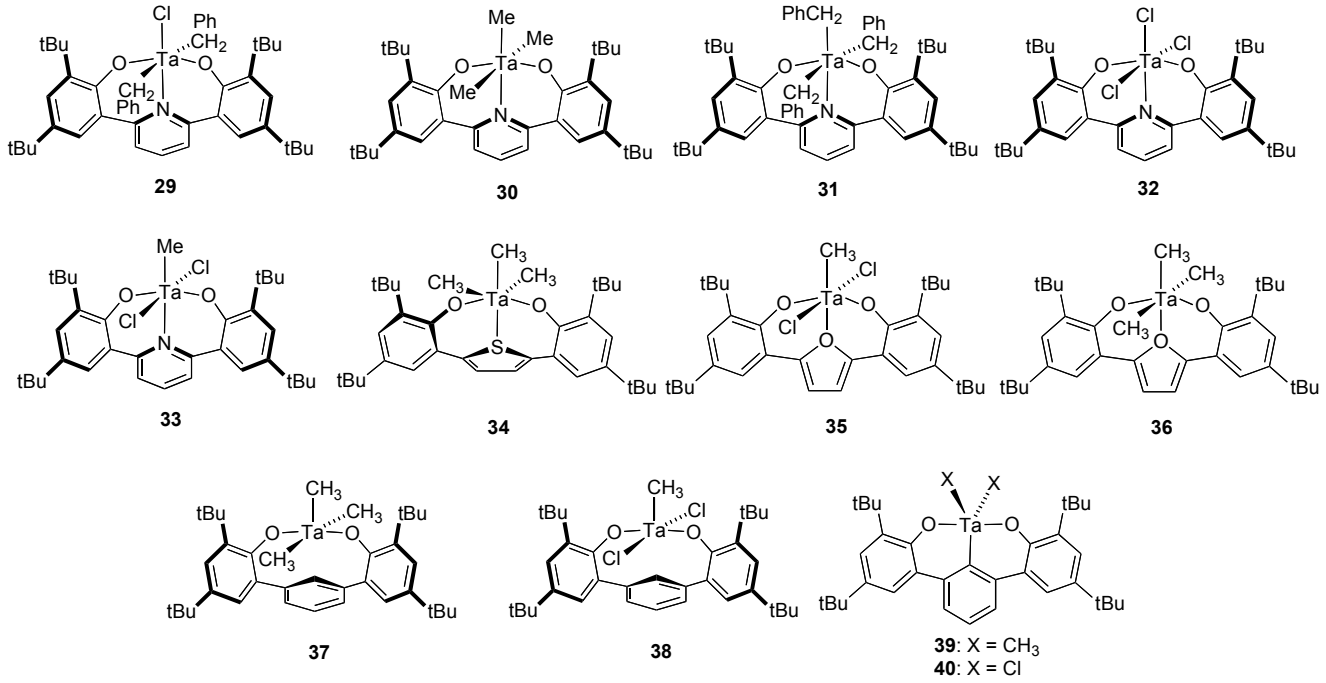

Solid-state structures of these complexes show that in all cases the ligands bind in a *mer* fashion, but with different geometries of the LX_2 frameworks. The pyridine-linked system (**29** – **33**) binds in a C_s-fashion, the furan-linked system (**35**, **36**) in a C_{2v}-fashion, and the thiophene linked system (**34**) in a C_1-fashion. A bis(phenolate)pyridine tantalum tribenzyl species (**31**), upon heating in the presence of dimethylphenylphosphine, generates a stable benzylidene complex by α-hydrogen abstraction with loss of toluene and PMe_2Ph trapping. This process was found to be independent of PMe_2Ph concentration with $\Delta H^{\ddagger} = 31.3 \pm 0.6$ kcal·mol^{-1} and $\Delta S^{\ddagger} = 3 \pm 2$ cal·mol^{-1}·K^{-1}, and the kinetic isotope effect $k_H/k_D = 4.9 \pm 0.4$, consistent with a mechanism involving rate determining α-hydrogen abstraction with loss of toluene, followed by fast phosphine coordination to the resulting benzylidene species.

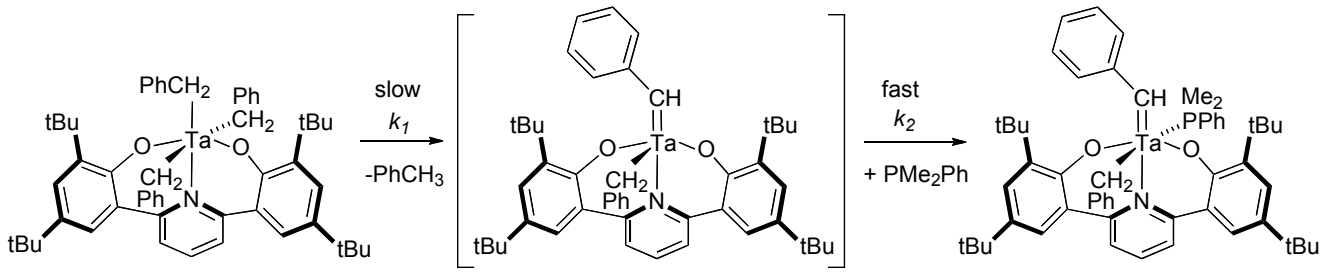

31

An X-ray structure determination reveals that the benzylidene π-bond is oriented perpendicular to the oxygen-oxygen vector forcing the phenyl and hydrogen toward *t*-butyl substituents of the phenolate groups, in accord with the prediction of DFT calculations, and reminiscent of the conformation of the corresponding benzylidene complex $Cp_2Ta(CHPh)(CH_2Ph)$, reported by Schrock and coworkers, where the sterically less crowded conformer is also the most stable.[44]

Tantalum alkyl complexes with the benzene-linked bis(phenolate) ligand ($Ta(CH_3)_2[(OC_6H_2\text{-}tBu_2)_2C_6H_3]$ (**37**), $Ta(CH_2Ph)_2[(OC_6H_2\text{-}tBu_2)_2C_6H_3]$, and $TaCl_2CH_3[(OC_6H_2\text{-}tBu_2)_2C_6H_4]$ (**38**)) are obtained with (to afford pincer complexes) or without cyclometallation at the *ipso*-position. Deuterium labeling of the phenol hydrogens and of the linking 1,3-benzene-diyl ring reveals an unexpected mechanism for metallation of bis(phenol)benzene with $TaCl_2(CH_3)_3$ to generate **38**. This process involves protonolysis of a methyl group, followed by C-H/Ta-CH_3 σ bond metathesis leading to cyclometallation of the linking ring, and finally protonation of the cyclometallated group by the pendant phenol.[45]

Scheme 11

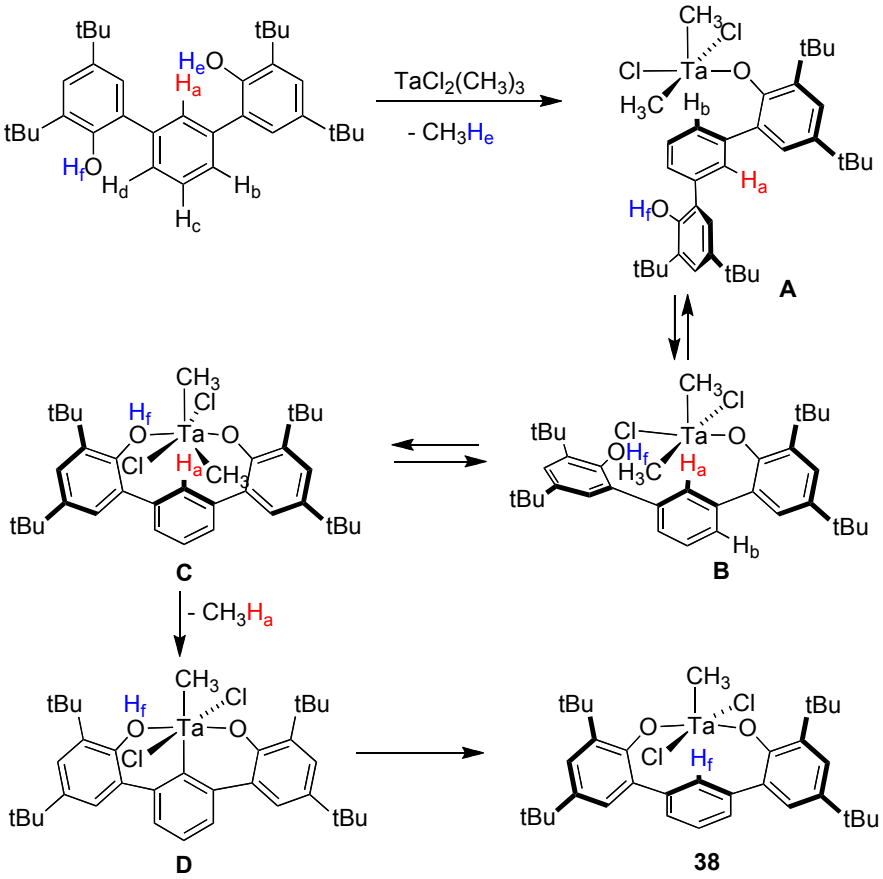

$TaCl_2CH_3[(OC_6H_2\text{-}tBu_2)_2C_6H_4]$ was found to undergo σ bond metathesis at temperatures over 90 °C to give the pincer complex $TaCl_2[(OC_6H_2\text{-}tBu_2)_2C_6H_3]$ (**40**) and methane ($\Delta H^{\ddagger} = 27.1 \pm 0.9$ kcal·mol^{-1}; $\Delta S^{\ddagger} = -2 \pm 2$ cal·mol^{-1}·K^{-1}, $k_H/k_D = 1.6 \pm 0.2$ at 125 °C). $Ta(CH_3)_2[(OC_6H_2\text{-}tBu_2)_2C_6H_3]$ (**39**) was found to react with tBuNC to insert into the Ta-CH_3 bonds and generate an imino-acyl species. Reaction of **39** with Ph_2CO or PhCN leads to insertion into the Ta-Ph bond. Among these complexes the ligand geometry varies leading to C_{2v}-, *pseudo*-C_s-, *pseudo*-C_2-, and C_1-symmetric structures.

(*xiii*). ***Alkylaluminum-Complexed Zirconocene Hydrides: Identification of Hydride-Bridged Species by NMR Spectroscopy.*** Together with Professor (Emeritus) Hans Brintzinger (University of Konstanz) we have undertaken some collaborative studies of the speciation of functioning zirconocene-based propylene polymerization catalyst systems, with particular attention to aluminum alkyl adducts of zirconocene hydrides.[46] The structures of three zirconocene aluminohydride clusters formed from the reactions of zirconocene dichlorides with diisobutylaluminum hydride (HAl^iBu_2), and determination of the factors that lead to preferential formation of each structure have been addressed, primarily by NMR characterization.

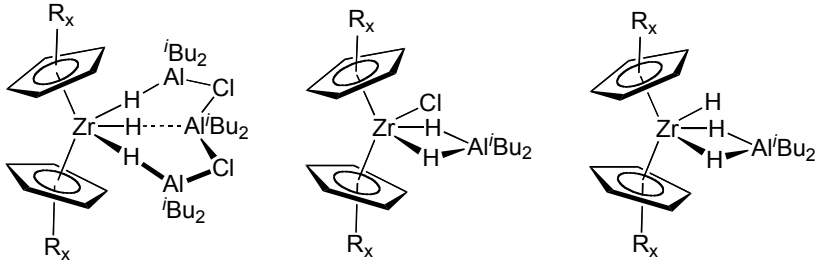

Reactions of unbridged zirconocene dichlorides, $(R_nC_5H_{5-n})_2ZrCl_2$ (n = 0, 1 or 2), with diisobutylaluminum hydride (HAl^iBu_2) result in the formation of tetranuclear trihydride clusters of the type $(R_nC_5H_{5-n})_2Zr(\mu\text{-}H)_3(Al^iBu_2)_3(\mu\text{-}Cl)_2$ (**[$ZrH_3Al_3Cl_2$]**), which contain three $[Al^iBu_2]$ units. Ring-bridged *ansa*-zirconocene dichlorides, $Me_2E(R_nC_5H_{4-n})_2ZrCl_2$ with E = C or Si, on the other hand, are found to form binuclear dihydride complexes of the type $Me_2E(R_nC_5H_{4-n})_2Zr(Cl)(\mu\text{-}H)_2Al^iBu_2$ (**[$ZrH_2Al_1Cl_1$]**) with only one $[Al^iBu_2]$ unit. More sterically encumbered *ansa*-zirconocene dichlorides react to generate the related (**[ZrH_3Al_1]**) unit. **[$ZrH_3Al_3Cl_2$]** is formed by non-bridged metallocenes {*e.g.* Cp_2ZrCl_2, $(C_5H_4TMS)_2ZrCl_2$, $(C_5H_4{}^nBu)_2ZrCl_2$, $(C_5H_4Me)_2ZrCl_2$ and $(1,2\text{-}C_5H_4Me_2)_2ZrCl_2$}, as well as *ansa*-metallocenes which have a C_2-bridge but low steric demand {*e.g.* $C_2H_4(C_5H_4)_2ZrCl_2$ and $C_2Me_4(C_5H_4)_2ZrCl_2$}. **[ZrH_3Al_1]** is formed by sterically encumbered *ansa*-metallocenes {e.g. *rac*-$Me_2Si(2\text{-TMS-}4\text{-}Me_3C\text{-}C_5H_2)_2ZrCl_2$ and *meso*-$Me_2Si(3\text{-}Me_3C\text{-}C_5H_3)_2ZrCl_2$}. Moreover, less sterically encumbered ligands can lead to **[ZrH_3Al_1]** when starting from the dihydride as opposed to the dichloride {*e.g.* *rac*-$[C_2H_4(1\text{-indenyl})_2ZrH_2]_2$}. **[$ZrH_2Cl_1Al_1$]** is formed by *ansa*-metallocenes that do not fall into either of the two previous categories {*e.g.* *rac*-$Me_2Si(1\text{-indenyl})_2ZrCl_2$, *rac*-$C_2H_4(1\text{-indenyl})_2ZrCl_2$, $Me_2(C_5H_4)_2ZrCl_2$, $Me_2Si(C_5H_4)_2ZrCl_2$, $Me_2Si(2,4\text{-}Me_2\text{-}C_5H_2)_2ZrCl_2$, $(Me_2Si)_2(C_5H_3)_2ZrCl_2$, $(Me_2Si)_2(2,4\text{-}{}^iPr_2\text{-}C_5H_1)(C_5H_3)ZrCl_2$, *rac*-$C_2H_4(4,5,6,7\text{-tetrahydroindenyl})_2ZrCl_2$, *rac*-$Me_2C(1\text{-indenyl})_2ZrCl_2$ and *meso*-$Me_2C(1\text{-indenyl})_2ZrCl_2$}.

The dichotomy between unbridged and bridged zirconocene derivatives with regard to tetranuclear *vs*. binuclear product formation is proposed to be related to different degrees of rotational freedom of their C_5-ring ligands. Alkylaluminum-complexed zirconocene dihydrides with a terminal Zr-Me group, such as $Me_2Si(ind)_2Zr(Me)(\mu\text{-}H)_2Al^iBu_2$ proved inaccessible, probably due to instability toward loss of methane. Species of this kind, observed in zirconocene-based catalyst systems activated by methylalumoxane (MAO), are proposed to be stabilized by interaction of their terminal Me group with a Lewis-acidic site of MAO. These species are of interest as regards to the number of active sites, because they may be dormant or resting states in metallocene-based olefin polymerizations (*vide infra*).

(*xiv*). ***Intramolecular C-H activation in the metallation of benzene-linked bis(phenolate)bis(benzyl) complexes of Ti, Zr, and Hf.*** As discussed above, although complexes **27** and **28** afford atactic polypropylene (not stereoregular PP) with only moderate activities upon activation with MAO, we did note a very clean and interesting fundamental transformation at higher temperatures: loss of toluene and formation of the dimeric pincer-ligated titanium mono-benzyl product (Scheme 13).

Scheme 13

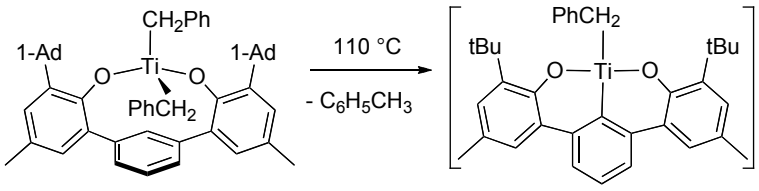

27

{Ti(CH$_2$C$_6$H$_5$)[(OC$_6$H$_2$-2-CMe$_3$-4-CH$_3$)C$_6$H$_3$(2-CMe$_3$-4-CH$_3$C$_6$H$_2$-μ$_2$-O]}$_2$

41

cf.

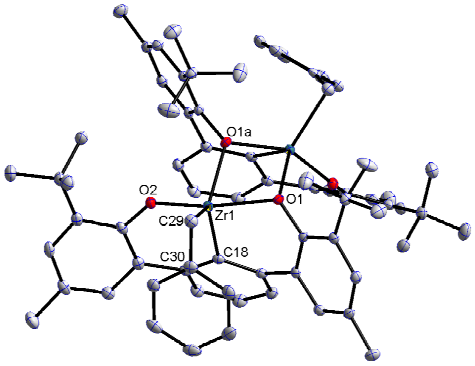

43

We undertook some mechanistic studies of this process for the **27**, as well as for the analogous zirconium (**42**) and hafnium (**44**) complexes.

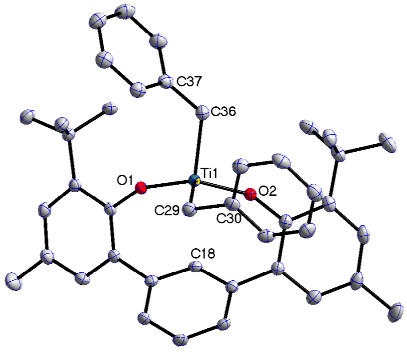

27

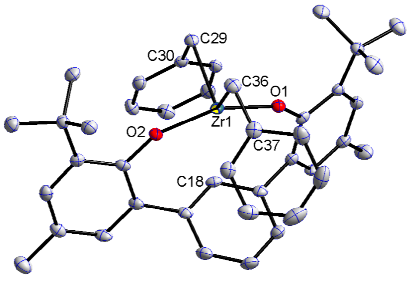

42

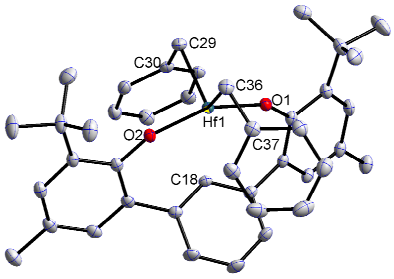

44

All three complexes are *pseudo*-tetrahedral with the position of the benzyl groups rotating slightly (about the M-C29 or M-C36 bonds) as the size of the metal increased. The O1-M-O2

angle increases from titanium to zirconium or hafnium, corresponding with the increase in metal size. Another interesting feature of these complexes was that although the C29-M-C36 angle remained quite constant, the M-C29-C30 and M-C36-C37 angles were more acute for zirconium and hafnium than titanium, implying these are more towards η^2-benzyls. None of these complexes shows a bond between the metal and C18; however, that distance is significantly greater for titanium than zirconium or hafnium (2.9 Å *vs* 2.7 Å).

Heating solutions of dibenzyl complexes **27**, 4**2**, or **44** in an aromatic solvent facilitated C-H bond activation to give toluene, presumably to form the corresponding cyclometallated species which readily dimerizes, as shown for **27** in Scheme 13. These metallation reactions are quite clean with no sign of decomposition or side products and thus are amenable to mechanistic study. Kinetics experiments for **27** reveal first order conversions with k_{obs} = 6.8 x 10^{-5}, 2.0 x 10^{-4}, and 4.6 x 10^{-4} s^{-1} at 378 K, 388 K, and 398K, respectively.

Perhaps the most striking observations concern the results of experiments designed to establish kinetic deuterium isotope effects. Two partially deuterated isotopologs of **27** were prepared: **27-*d*$_3$** and di(perdeuterato-benzyl) complex (**27-*d*$_{14}$**), following procedures analogous to those used to prepare previously described tantalum and hafnium complexes.[47]

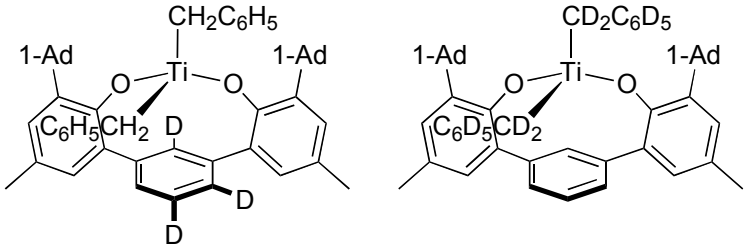

27-*d*$_3$ **27-*d*$_{14}$**

At 388 K the reaction rate for **27-*d*$_3$** is essential identical to that fo **27** (k_{obs} = 1.9 x 10^{-4} and 2.0 x 10^{-4} s^{-1}), while the rate of **27-*d*$_{14}$** was less than half the rate of **27** (k_{obs} = 8.0 x 10^{-5} and 2.0 x 10^{-4} s^{-1}), corresponding to a KIE (k_H/k_D) of 2.5. Moreover, both protio- (*i.e.* d_0) and monodeutero-toluene ($CDH_2C_6H_5$) were formed in a ratio of 1.3 to 1 from the reaction with **27-*d*$_3$** and both CH_2 and CHD in the benzyl groups of the dimer were observed (^{1}H NMR).

The fact that no KIE was observed with **27-*d*$_3$** (as well as the formation perprotio and partially deuterated benzyls of product **41**) argues against a straightforward, concerted σ-bond metathesis elimination of toluene by abstraction of hydrogen from the 2-position of the benzene-1,3-diyl linker by a benzyl group of **27**. The observed KIE with **27-*d*$_{14}$** implies that either α-abstraction of benzyl protons (to generate a Ti-benzylidene intermediate) or *ortho*-abstraction of an aromatic hydrogen (to generate a

benzotitanacyclobutane intermediate) is the likely rate-determining step. Both of these mechanisms have been identified in the thermal decomposition of $Cp^*_2Hf(CH_2C_6H_5)_2$.[53]

(*xv*). ***New, More Stereorigid LX_2-Pincer Ligand Systems for Early Transition Metal Chemistry and Catalysis.*** We undertook a major program aimed at exploring the potential of non-metallocene complexes of early transition metals to effect stereoselective transformations, particularly α-olefin polymerizations. We noted that both C_2- and C_s-symmetric complexes of the group 4 transition metal precursors were obtained. The factors dictating one geometry over the alternative were not obvious. To further develop the organometallic chemistry of early transition metals supported by these pincer ligands, a series of tantalum amine, amido, and imido complexes has been synthesized.[48] As discussed below, these tantalum complexes have been particularly instructive for elucidating the importance of phenolate-metal π-bonding on the preferred [(ONO)Ta] symmetry and have provided insights into the differences between the [(ONO)Ta] and [Cp_2Ta] platforms.

Reaction of (ONO)$TaMe_3$ (ONO = pyridine-2,6-*bis*(4,6-^{t}Bu$_2$-phenolate)) with three equivalents of aniline at 90 °C over the course of 12 hours yields the amino-amido-imido tantalum complex, (ONO)Ta(NH_2Ph)(NHPh)(NPh) (**45**).

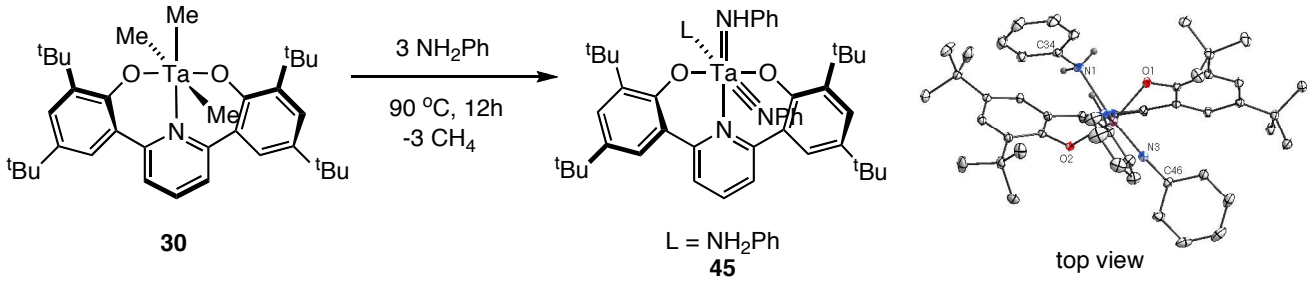

30 L = NH_2Ph **45**

Ta-N bond lengths for **45** are indicative of three types of Ta-N bonding: 2.480(1) Å for the L-type aniline; 2.027(1) Å for the LX-type anilide; and 1.786(1) Å for the LX_2-type phenylimide. The meridional binding mode of the [ONO] ligand is typical for early metal complexes of the *bis*(phenolate)pyridine ligand; however, it is the first six-coordinate tantalum complex to exhibit a C_2-twisted binding rather than the typical C_s-folded mode as for **30**. The average Ta-O bond distance in **45** is 2.002(1) Å, which is significantly (~ 0.1 Å) longer than the distances observed earlier.[47] These structural features prompted a further investigation of the underlying reasons for a preference for C_2 versus C_s ligand geometry.

A distinctive feature of **45** (an "(ONO)Ta(L)(LX)(LX_2)-type" complex), as opposed to all previously studied (ONO)TaX_3 complexes, is presence of three strong Ta-X π bonds, one for the amido and two for the imido ligand. We therefore hypothesized that these Ta-N π bonds

were responsible for the observed C_2 rather than C_s ligand geometry. A series of [(ONO)Ta] amides and imides with varying X-type, LX-type, and LX_2-type ligands, and hence differing numbers Ta-N of π-bonds, were synthesized.

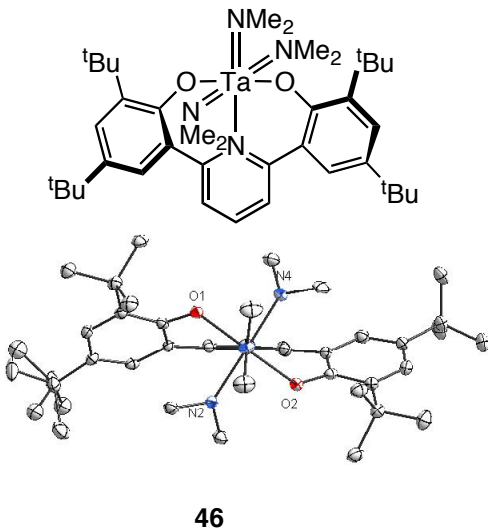

46

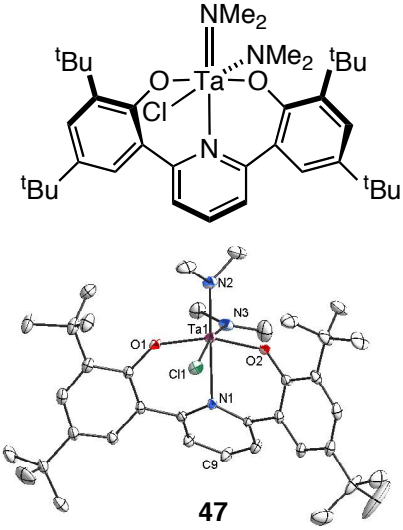

47

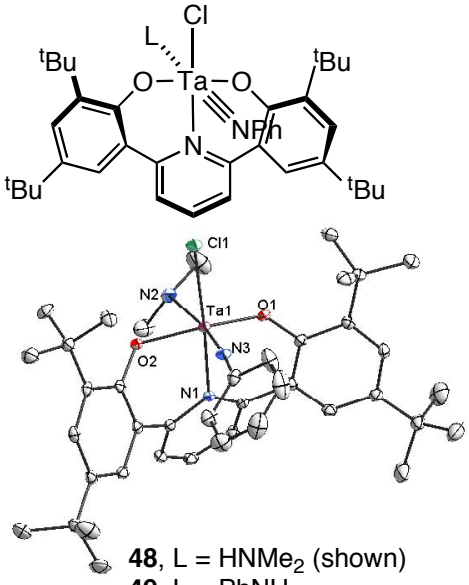

48, L = $HNMe_2$ (shown)
49, L = $PhNH_2$

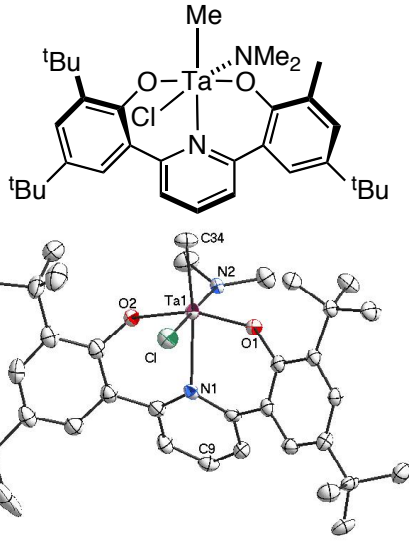

50

From the structural data for these complexes, as well as for other previously reported tantalum complexes having the *bis*(phenolate)pyridine ancillary ligand, it is apparent that the number of strong tantalum-nitrogen π bonds for the remaining three ligands significantly affects the degree of Ta-O π bonding for two phenolates. The amount of Ta-O π bonding can be quantified by examining the distances in the solid-state structures (Table 1). In complexes where there is no π bonding associated with the remaining ligands, *i. e.* they are X-type, the average Ta-O bond length is roughly 1.9 Å. As the number of π-bonding ligands is

increased, a corresponding increase in Ta-O bond length is also observed, reaching as high as 2.0 Å in cases where there are three strong π-donating ancillary ligands, as for example is the case with **45** (L, LX, and LX_2 ligands) and **46** (three LX ligands). Thus, it is apparent that the Ta-O bond order decreases as additional strong π bonders are introduced into the system—going from a Ta-O bond order of 2 in the case of zero π donating ligands down to an order of 1 when there are three strong π donating ligands. The rather small change in the Ta-O bond length over all of the compounds (~0.1 Å) is likely due to generally poor π donating ability of electronegative oxygen and the inherent rigidity of the system, which should attenuate the overall change in bond lengths.

Table 1. Observed solid-state ligand symmetries and average Ta-O bond length in selected tantalum (*bis*)phenolate complexes.

L_3 for (ONO)TaL_3	Symmetry	#of Ta=L π bonds	Average Ta-O bond order[a]	d(Ta-O)$_{ave}$ (Å)
(NPh)(NHPh)(NH_2Ph) (**45**)	C_2	3	1	2.002(1)
(NMe_2)$_3$ (**46**)	C_2	3	1	1.985(2)
(NMe_2)$_2$Cl (**47**)	C_s	2	1.5	1.924(3)
(NPh)(HNMe_2)Cl (**48**)	C_s	2	1.5	1.954(2)
(NPh)(NH_2Ph)Cl (**49**)	C_s	2	1.5	1.948(3)[b]
(NMe_2)(CH_3)Cl (**50**)	C_s	1	2	1.887(2)
(=CHPh)(CH_2Ph)(PR_3)	C_s	1	2	1.922(1)
(CH_3)$_3$ (**30**)[b]	C_s	0	2[d]	1.906(1)

[a]To complete the 18 electron count at Ta. [b]16 electron maximum.

From a molecular orbital perspective, a C_s-symmetric *bis*(phenolate)pyridine ligand should be able to π bond to the metal center through both of the lone pairs on each oxygen (although the two "lone pairs" are of differing energy), making bonds with d_{xz} and d_{xy} on tantalum (Scheme 14). In the case of the *mono*(amide) **50** and the previously reported benzylidene complex,[47] where there exists only one ligand π bond, these Ta-O π interactions force the benzylidene (or amide) ligand to π bond with d_{yz} generating an 18-electron complex, despite the consequence of forcing the phenyl ring of the benzylidene toward a phenolate *tert*-butyl group. However, in the case where there are two ligand N-to-Ta π bonds such as the *bis*(amide) **47** or the phenylimide-chlorides **48** and **49**, one of the two Ta-O π bonds must be sacrificed to make the second ligand π bond (Scheme 14); the remaining Ta-O π interaction occurs through d_{xz}.

Scheme 14

0 or 1(shown) strong Ta-N π bonds

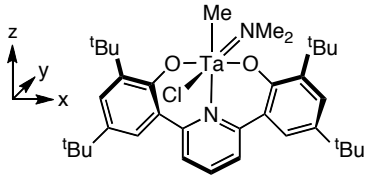

50
(similarly for (ONO)Ta(=CHPh)(CH$_2$Ph)(PR$_3$))

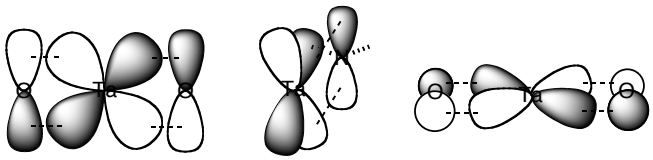

2 strong Ta-N π bonds:

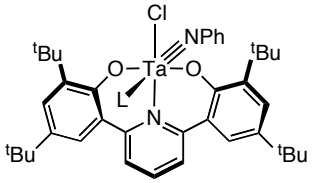

48, **49**
(similarly for **47**)

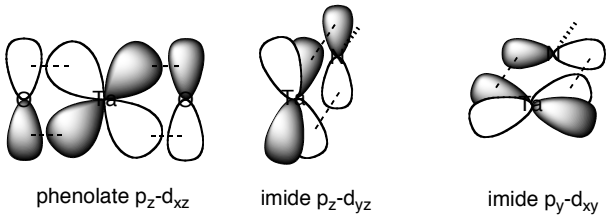

3 strong Ta-N π bonds:

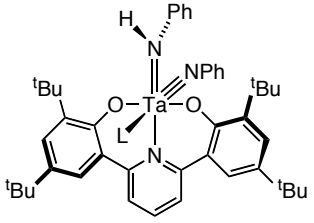

45
(similarly for **46**)

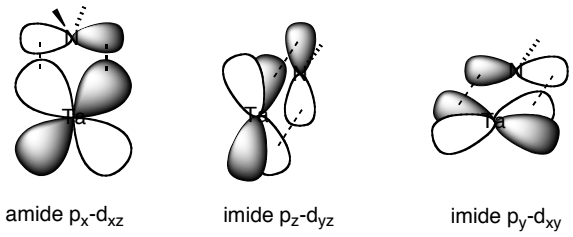

Finally, in the case where there are three strong ligand π bonds (**45** and **46**), all Ta-O π bonding is precluded to accommodate π bonding to the other LX and LX$_2$ ligands. In these cases, the *bis*(phenolate) ligand twists from C_s-symmetry to C_2-symmetry. This symmetry switch is likely due to two factors. Firstly, switching to a C_2-symmetric arrangement reduces overlap between the phenolate filled oxygen p orbitals and the now filled N-to-Ta π oribitals, reducing filled-filled repulsions. Secondly, this twist is likely a geometric relaxation effect; the C_2-symmetry can better accommodate the large tantalum atom because twisting lengthens the Ta-O bonds. The less than optimal binding pocket of the *bis*(phenolate)pyridine in the C_s-symmetric geometry increases strain on the ring system—as evidenced by the canted pyridine. The implication of either explanation is that any phenolate π-bonding requires and enforces a C_s-symmetric binding.

DFT calculations (B3LYP, 6-31G**, LANL2DZ Ta pseudopotential) performed on **45** support the extent of Ta-N π bonding, very different from its earlier-reported metallocene counterpart Cp*$_2$Ta(=NPh)(H).[49] In order to examine potential steric interactions as

contributing factors to the preferred geometry DFT calculations were performed on less crowded models for complexes in Table 1: the phenolate substituents were removed for (ONO)Ta(NH_3)(NH_2)(NH) and (ONO)Ta(NMe_2)$_3$, and for (ONO)Ta(NH_2)$_2$Cl, (ONO)Ta(NH_3)(NH)Cl, and (ONO)Ta(NMe_2)$_2$Cl. These revealed optimized structures with the observed symmetries in all cases. Hence, the preferred geometry appears to be determined by the degree of Ta-O π bonding with the phenolate ligands. When Ta-O π bonds are required to complete the 18-electron count, the *bis*(phenolate)pyridine ligand binds in a C_s-symmetric fashion. In cases where strong π donation with ancillary ligands precludes Ta-O π bonding (*i. e.*, when there are three strong π donor interactions from the other ligands), the *bis*(phenolate) ligand twists in a C_2 fashion either to reduce filled-filled repulsions between the Ta-X π bonds and the oxygen lone pairs and to a less strained (ONO) geometry. The important conclusion are that the *bis*(phenolate)donor pincer ligand, unlike cyclopentadienyls of the analogous metallocene systems, is not a strong enough π-donor to exert total control over the electronic and geometric properties of the complex.

(*xvi*). ***New Ti, Zr and Ta Complexes with LX_2 Ligands Having Anilide, Thiophenolate, and Phosphide X Type Ligands.*** In order to exploit our new understanding of the π-effects in these systems, we explored the use of stronger π-donor atoms in aryl-linked pincer complexes, *e.g. bis(*anilide)-, *bis*(thiophenolate)- and *bis*(phosphide)donor analogs of the *bis*(phenolate)donor ligand. We originally anticipated that the stronger π-donor X groups of these LX_2 pincer ligands would dominate the complexes' geometry, and enforce C_s symmetry, even when ancillary ligands are potentially π-bonding. Catalysts with stronger pincer ligand π-bonding should be more rigid than those with the *bis*(phenolate)pyridine scaffold, and their use in polymerizations and other transformations should provide a more predictable catalyst structure. In this regard they should more closely resemble metallocenes.

(a) ***Zirconium and Titanium Propylene Polymerization Precatalysts Supported by a Fluxional C_2-Symmetric Bis(anilide)pyridine Ligand.*** Titanium and zirconium complexes supported by a *bis*(anilide)pyridine ligand (NNN = pyridine-2,6-*bis(*N-mesitylanilide)) were synthesized and crystallographically characterized. C_2 symmetric *bis*(dimethylamide) complexes were generated from aminolysis of M(NMe_2)$_4$ with the neutral, diprotonated NNN ligand or by salt metathesis of the dipotassium salt of NNN with M(NMe_2)$_2$$Cl_2$. In contrast to previously reported pyridine *bis*(phenoxide) complexes, the ligand geometry of these complexes appears to be dictated by chelate ring strain rather than metal-ligand π-bonding. The crystal structures of the 5-coordinate dihalide complexes (NNN)MCl_2 (M = Ti, Zr) display a C_1-symmetric geometry with a stabilizing *ipso* interaction between the metal and the anilido ligand. Coordination of THF to (NNN)$ZrCl_2$ generates a 6-coordinate C_2-

symmetric complex. Facile antipode interconversion of the C_2 complexes, possibly via flat, C_{2v} intermediates, has been investigated by variable temperature ^{1}H NMR spectroscopy for (NNN)$MX_2(THF)_n$ (M = Ti, Zr; X = NMe_2, Cl) and (NNN)$Zr(CH_2Ph)_2$. These complexes were tested as propylene polymerization precatalysts, with most complexes giving low to moderate activities (10^2 - 10^4 g/mol·h) for the formation of stereo-irregular polypropylene.

(b) ***Synthesis of a Bis(thiophenolate)pyridine Ligand and its Titanium, Zirconium, and Tantalum Complexes.*** A precursor to a new tridentate LX_2 type ligand, bis(thiolphenol)pyridine ((SNS)H_2 = (2-$C_6H_4SH)_2$-2,6-C_5H_3N), was prepared. Bis(thiolphenolate)pyridine complexes of Ti, Zr, and Ta having dialkylamido coligands were synthesized and structurally characterized. The zirconium complex, (SNS)$Zr(NMe_2)_2$ (**4**), displays C_2 symmetry in the solid state, unlike the related bis(phenolate)pyridine compound, C_s-symmetric (ONO)$Ti(NMe_2)_2$. This change is likely the result of strain about the sulfur atom in the six membered chelate with longer metal-sulfur and carbon-sulfur bonds. Solid-state structures of tantalum complexes (SNS)$Ta(NMe_2)_3$ (**5**) and (SNS)$TaCl(NEt_2)_2$ (**6**) also display pronounced C_2 twisting of the SNS ligand. 1D and 2D NMR experiments confirm that **5** retains C_2 symmetry in solution, and equivalencing of the equatorial amide methyl groups likely occurs by hindered rotation about the Ta-N bonds. The fluxional behavior of **6** in solution was studied by variable temperature ^{1}H NMR. Observation of separate signals for the diastereotopic protons of the methylene unit of the diethylamide indicates that the complex remains locked on the NMR timescale in one diastereomeric conformation at temperatures below -50 °C. At higher temperatures equilibration of diastereomeric methylene protons occurs via a process that interconverts antipodes.

(c) ***A Novel Bis(phosphido)pyridine [PNP](2-) Pincer Ligand and Its Potassium and Bis(dimethylamido)zirconium(IV) Complexes.*** A novel PNP pincer bis(secondary-phosphine)pyridine ligand, 2,6-bis(2-(phenylphosphino)phenyl)pyridine, has been prepared in high yield, and the properties of the doubly deprotonated form as a ligand for $K_4(PNP)_2(THF)_6$ and (PNP)$Zr(NMe_2)_2$ have been investigated. The neutral PNP ligand is isolated as a mixture of non-interconverting diastereomers due to the presence of two chirogenic phosphorus atoms, but coordination of the dianionic form to potassium and zirconium allows for isolation of a single diastereomer in near quantitative yield. The structure of a bis(dimethylamido)zirconium(IV) derivative of the bis(phoshido)pyridine ligand and DFT calculations suggest that the phosphides do not π-bond to early transition metals, likely due to geometric strain and possibly orbital size mismatch between phosphorus and zirconium. As a result, the soft phosphides are prone to formation of insoluble oligomers with substantial bridging of the phosphido lone pairs to other zirconium centers.

(*xvii*). ***(dme)MCl$_3$(NNPh$_2$) (dme = dimethoxyethane; M = Nb, Ta): A Versatile Synthon for [Ta=NNPh$_2$] Hydrazido(2-) Complexes.*** In the course of our work related to π-effects on *bis*(phenolate)pyridine ligands, we synthesized a novel tantalum hydrazido(2-) complex, (ONO)TaCl(py)(NNPh$_2$) (**54**) and (ONO)TaCl(HNMe$_2$)(NNMe$_2$) (**55**), only the second and third structurally characterized hydrazido(2-) tantalum complexes. Additional tantalum complexes with macrocyclic ligand systems have also been isolated very recently (Scheme 19).

Scheme 19

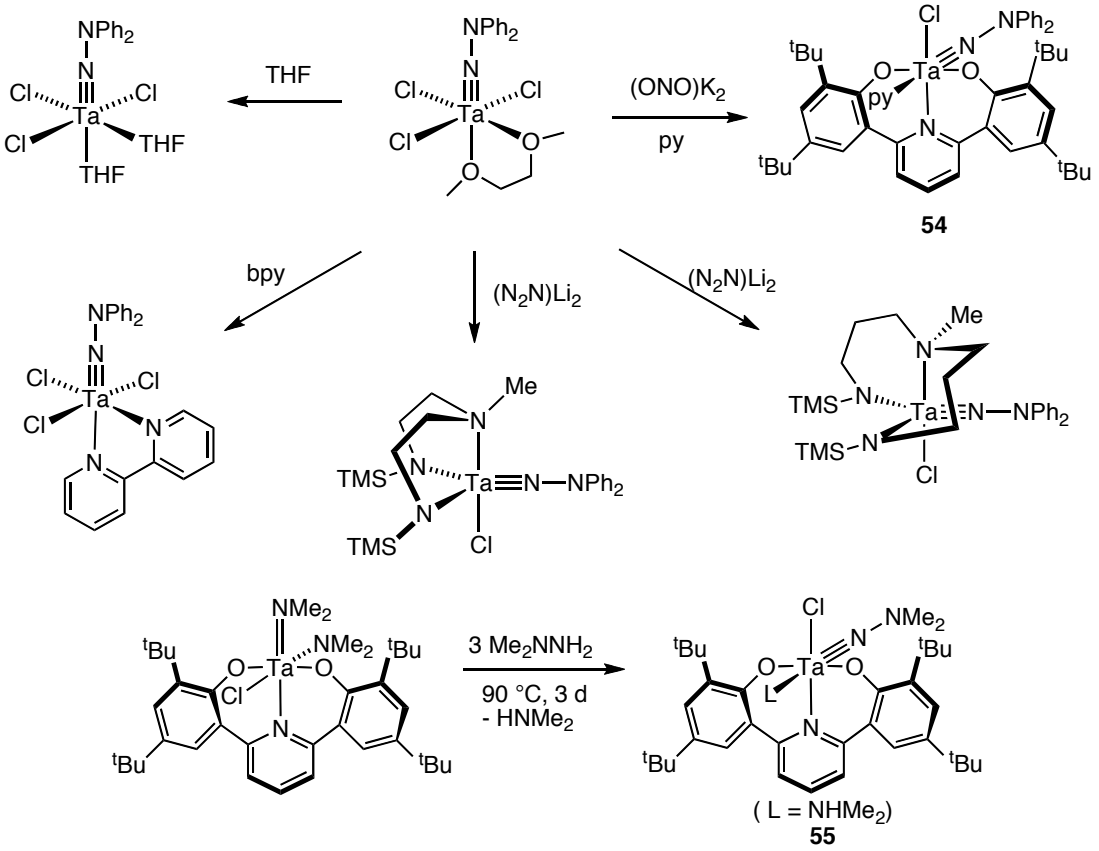

Their syntheses prompted us to explore the reactivity of this functional group, especially as it relates to hydrohydrazination or *bis*(amination). A particularly attractive feature is that it the chloride ligand should allow access to cationic hydrazido species via halide abstraction. We anticipate that these cationic complexes should be more reactive than their neutral group 4 counterparts, in accord with the electrophilic mechanism for *bis*(amination).

(*xviii*). ***Groups 5 and 6 Terminal Hydrazido(2-) Complexes: N$_\beta$ Substituent Effects on Ligand-to-Metal Charge-Transfer Energies and Oxidation States.*** Brightly colored terminal hydrazido(2-) (dme)MCl$_3$(NNR$_2$) (dme = 1,2-dimethoxyethane; M = Nb, Ta; R = alkyl or aryl) or (MeCN)WCl$_4$(NNR$_2$) complexes have been synthesized and characterized. Perturbing the electronic environment of the β (NR$_2$) nitrogen affects the energy of the lowest-energy charge

transfer transition in these complexes. For group 5 complexes, increasing the energy of the N_β lone pair decreases the LMCT energy, except for electron-rich Nb dialkylhydrazides, which pyramidalize N_β in order to reduce the overlap between the Nb=N_α π bond and the N_β lone pair. For W complexes, increasing the energy of N_β eventually leads to reduction from formally [W^{VI}≡N-NR_2] with a hydrazido(2-) ligand to [W^{IV}=N=NR_2] with a neutral 1,1-diazene ligand. The photophysical properties of these complexes highlight the potential redox non-innocence of hydrazido ligands that could lead to ligand- and/or metal-based redox chemistry in early transition metal derivatives.

(*xix*) ***Exploratory Reactivity Studies of Iron Derivatives Having a Pyridine-Linked Bis(anilide) Pincer Ligand.*** We developed the synthesis of a *bis*(anilide) variant of the *bis*(phenolate)pyridine ligands described above, along with some preliminary investigations of its coordination chemistry for iron.[50] The synthesis of the ligand precursor **56** was accomplished via *in situ* borylation of 2-bromoaniline, followed by a two-fold Suzuki coupling with 2,6-dibromopyridine. Arylation of **56** with an excess of mesityl bromide was accomplished with Buchwald-Hartwig coupling, yielding the ligand [**57**]H_2 (Scheme 20). An iron(II) derivative was readily obtained by deprotonation of [**57**]H_2 with $LiCH_2SiMe_3$ and treatment with $FeCl_2$ in THF solution, affording **58**. High spin **58** undergoes quasi-reversible electrochemical reduction and oxidation, suggesting that the (NNN) LX_2 framework is capable of supporting either reduced or oxidized species. Treatment with I_2 or O_2 results in clean oxidation to (NNN)Fe^{III}I (**59**) and dimeric [(NNN)Fe^{III}](μ_2-O) (**60**).

Scheme 20

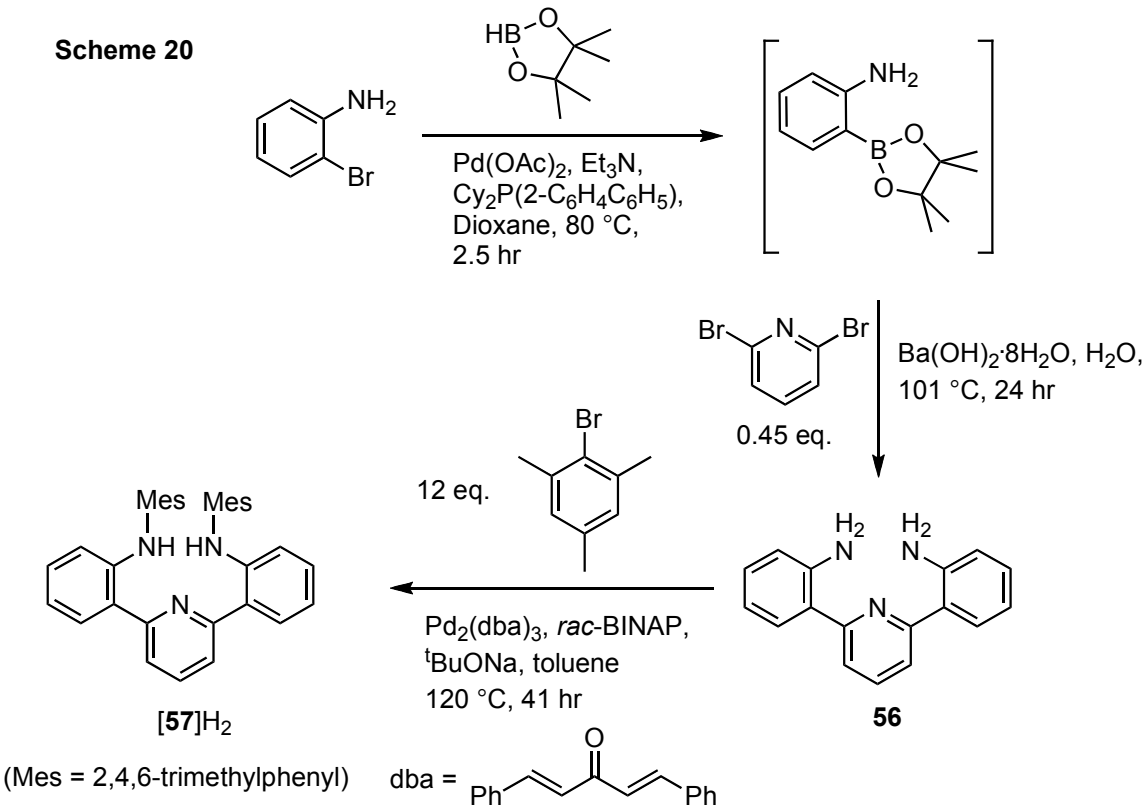

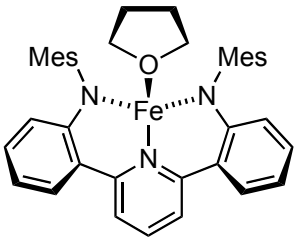

58

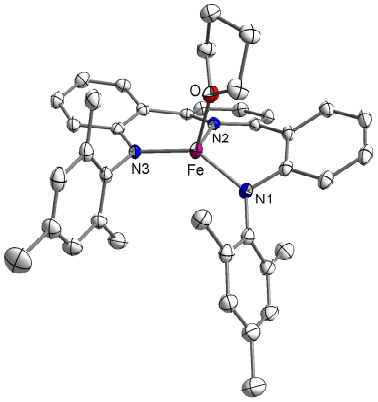

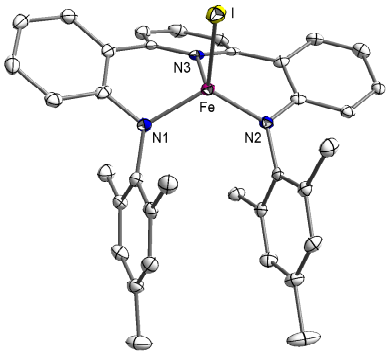

59

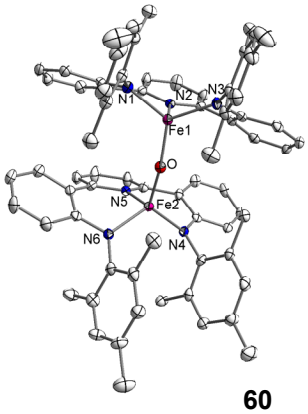

60

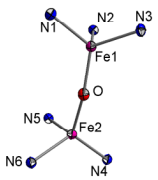

(*xx*). ***A Novel Type of Cationic Alkylaluminum-Complexed Zirconocene Hydrides: NMR-Spectroscopic Identification, Diffractometric Structure Determination and Interconversion with Other Zirconocene Cations.*** The *ansa*-zirconocene complex *rac*-Me_2Si(1-indenyl)$_2ZrCl_2$ ((SBI)$ZrCl_2$) reacts with diisobutylaluminum hydride and trityl tetrakis(perfluorophenyl)borate in hydrocarbon solutions to give the cation $[(SBI)Zr(\mu\text{-}H)_3(Al^iBu_2)_2]^+$, the identity of which is derived from NMR data and supported by a crystallographic structure determination. Analogous reactions proceed with many other zirconocene dichloride complexes. $[(SBI)Zr(\mu\text{-}H)_3(Al^iBu_2)_2]^+$ reacts reversibly with $ClAl^iBu_2$ to give the dichloro-bridged cation $[(SBI)Zr(\mu\text{-}Cl)_2Al^iBu_2]^+$. Reaction with $AlMe_3$ first leads to mixed-alkyl species $[(SBI)Zr(\mu\text{-}H)_3(AlMe_x{}^iBu_{2-x})_2]^+$ by exchange of alkyl groups between aluminum centers. At higher $AlMe_3$/Zr ratios, $[(SBI)Zr(\mu\text{-}Me)_2AlMe_2]^+$, a constituent of methylalumoxane-activated catalyst systems, is formed in an equilibrium with the hydride cation $[(SBI)Zr(\mu\text{-}H)_3(AlR_2)_2]^+$ strongly predominating at comparable HAl^iBu_2 and $AlMe_3$ concentrations, implicating the latter's presence in olefin polymerization catalyst systems.

(*xxi*). ***Titanium Complexes of a Pyridine-bis(phenolate) Ligand: Active Catalysts for Intermolecular Hydroamination or Cyclotrimerization of Alkynes.*** A class of titanium precatalysts of the type (ONO)TiX_2 (ONO = pyridine-2,6-*bis*(4,6-$(CMe_3)_2$-phenolate); X = Bn, NMe_2) have been synthesized and crystallographically characterized. The (ONO)TiX_2 complexes are highly active precatalysts for the intermolecular hydroamination of internal alkynes with primary arylamines and some alkylamines. A class of titanium imido complexes, (ONO)Ti(L)(NR) (L = $HNMe_2$, py; R = Ph, CMe_3) have also been synthesized and characterized and provide structural analogues to intermediates on the purported catalytic cycle. These imido complexes are also competent hydroamination precatalysts. When (ONO)$TiBn_2$ (**1**) is heated only in the presence of an electron-rich alkyne, alkyne cyclotrimerization is observed. During the cyclotrimerization reaction the Ti^{IV} precatalyst is reduced to Ti^{II}, which is the active species for catalysis. **1** represents a convenient and stable Ti^{IV} trimerization precatalyst and does not require an external reductant to initiate cyclotrimerization. A mechanism for the formation of Ti^{II} involving multiple alkyne insertions into a [Ti=NR] species is presented. An (ONO)Ti^{II} species generated from reduction of (ONO)$TiCl_2(HNMe_2)$ has been trapped by ethylene and crystallographically characterized.

(*xxii*). ***Investigations into Asymmetric Post-Metallocene Group 4 Complexes for the Synthesis of Highly Regioirregular Polypropylene.*** A series of asymmetric post-metallocene group 4 complexes based on a modular anilide(pyridine)phenoxide framework have been

synthesized and tested for propylene polymerization activity. These complexes, upon activation with methylaluminoxane (MAO), produce highly regioirregular and stereoirregular polypropylene with moderate to good activities. Surprisingly, modification of the anilide R-group substituent from 1-phenethyl to benzyl or adamantyl did not significantly change the polymer microstructure as determined by ^{13}C NMR spectroscopy. Although polymer molecular weights and polydispersities vary with propylene pressure, temperature, and activator, regio- and stereoirregularity were also found to be relatively insensitive to these variables. When the polymerization is conducted at 70 °C under dihydrogen, partial decomposition to a highly active catalyst that produces an isotactic microstructure occurs; the undecomposed catalyst continues to produce highly regioirregular and stereoirregular polypropylene under those conditions.

Publications of John E. Bercaw

2008-2014

Those that resulted solely or in part from DOE grant support:

232. Catalyst Site Epimerization during the Kinetic Resolution of Chiral α Olefins by Polymerization
Endy Y. Min, Jeffery A. Byers, and John E. Bercaw
Organometallics **2008**, *27*, 2179-2188.

233. Transition Metal Catalysts
Stefan Spitzmesser, Paul R. Elowe, and John E. Bercaw
International Patent Classification: B01J 31/18 (2006.01), August 9, 2007.

236. Zirconium and Titanium Complexes Supported by Tridentate LX_2 Ligands having Two Phenolates Linked to Furan, Thiophene, and Pyridine Donors: Precatalysts for Propylene Polymerization and Oligomerization
Theodor Agapie, Lawrence M. Henling, Antonio G. DiPasquale, Arnold Rheingold, and John E. Bercaw
Organometallics **2008**, *27*, 6245-6256.

237. Synthesis and Reactivity of Tantalum Complexes Supported by Bidentate X_2 and Tridentate LX_2 Ligands having Two Phenolates Linked to Pyridine, Thiophene, Furan, and Benzene Connectors – Mechanistic Studies of the Formation of a Tantalum Benzylidene and Insertion Chemistry for Tantalum-Carbon Bonds
Theodor Agapie, Michael W. Day, and John E. Bercaw
Organometallics **2008**, *27*, 6123-6142.

243. Alkylaluminum-Complexed Zirconocene Hydrides: Identification of Hydride-Bridged Species by NMR Spectroscopy
Steven M. Baldwin, John E. Bercaw, and Hans-Herbert Brintzinger
J. Am. Chem. Soc. **2008**, *130*, 17423-17433.

245. Synthesis and Characterization of Iron Derivatives Having a Pyridine-Linked Bis(anilide) Pincer Ligand
Edward C. Weintrob, Daniel Tofan, and John E. Bercaw
Inorg. Chem. **2009**, *48*, 3808-3813.

246. Solvent, Additive and Co-Catalyst Effects for Ethylene Oligomerization Catalysis
Paul R. Elowe and John E. Bercaw
International Patent Classification: C07C 2/08 (2006.01), April 9, 2009.

247. Amine, Amido, and Imido Complexes of Tantalum Supported by a Pyridine-Linked Bis(phenolate) Pincer Ligand. Ta-N π Bonding Influences Pincer Ligand Geometry
Ian A. Tonks, Larry M. Henling, Michael W. Day and John E. Bercaw
Inorg. Chem., **2009**, *48*, 5096-5105.

254. Synthesis of Early Transition Metal Bisphenolate Complexes and their Use as Olefin Polymerization Catalysts
Suzanne R. Golisz and John E. Bercaw
Macromolecules **2009**, *42*, 8751-8762.

263. $(dme)MCl_3(NNPh_2)$ (dme = dimethoxyethane; M = Nb, Ta): A Versatile Synthon for $[Ta{=}NNPh_2]$ Hydrazido(2-) Complexes
Ian A. Tonks and John E. Bercaw
Inorg. Chem. **2010**, *49*, 4648-4656.

264. Intramolecular C-H Activation of a Bisphenolate(benzene) ligand for a Titanium Dibenzyl Complex. Competing Pathways Involving a-Hydrogen Abstraction and s-Bond Metathesis
Suzanne R. Golisz, Jay A. Labinger, and John E. Bercaw
Organometallics, **2010**, *29*, 5026-5032.

265. Cationic Alkylaluminum-Complexed Zirconocene Hydrides as Participants in Olefin-Polymerization Catalysis
Steven M. Baldwin,† John E. Bercaw, Lawrence M. Henling, Michael W. Day, and Hans H. Brintzinger
J. Am. Chem. Soc. **2010**, *132*, 13969-13971.

266. A Novel Type of Cationic Alkylaluminum-Complexed Zirconocene Hydrides: NMR-Spectroscopic Identification, Diffractometric Structure Determination and Interconversion with Other Zirconocene Cations
Steven M. Baldwin, John E. Bercaw, and Hans H. Brintzinger
J. Am. Chem. Soc., **2011**, *133*, 1805-1813.

270. A Novel Bis(phosphido)pyridine [PNP](2-) Pincer Ligand and Its Potassium and Bis(dimethylamido)zirconium(IV) Complexes
Matthew S. Winston and John E. Bercaw
Organometallics, **2010**, *29*, 6408-6416.

277. Zirconium and Titanium Propylene Polymerization Precatalysts Supported by a Fluxional C_2-Symmetric Bis(anilide)pyridine Ligand
Ian A. Tonks, Daniel Tofan, Edward C. Weintrob, Theodor Agapie, and John E. Bercaw
Organometallics, **2012**, *31*, 1965-1974.

278. Groups 5 and 6 Terminal Hydrazido(2-) Complexes: N_β Substituent Effects on Ligand-to-Metal Charge-Transfer Energies and Oxidation States
Ian A. Tonks, Alec Durrell, Harry B. Gray, and John E. Bercaw
J. Am. Chem. Soc., **2012**, *134*, 7301-7304.

280. Highly Regioirregular Polypropylene from Asymmetric Group 4 Anilide(pyridine)phenoxide Complexes
Rachel C. Klet, David G. VanderVelde, Jay A. Labinger and John E. Bercaw
Chem. Comm., **2012**, *48*, 6657-6659.

283. Activator-Free Olefin Oligomerization and Isomerization Reactions Catalyzed by Air- and Water-Tolerant Wacker Oxidation Intermediate
Matthew S. Winston, Paul F. Oblad, Jay A. Labinger, John E. Bercaw
Angew. Chem. Int. Ed. Engl. **2012**, *51*, 9822.

285. Synthesis of a Bis(thiophenolate)pyridine Ligand and Its Titanium, Zirconium, and Tantalum Complexes
Taylor N. Lenton, David G. VanderVelde, and John E. Bercaw
Organometallics, **2012**, *31*, 7492-7499.

286. Unexpected Rearrangements in the Synthesis of an Unsymmetrical Tridentate Dianionic N-Heterocyclic Carbene
Emmanuelle Despagnet-Ayoub, Karinne Miqueu, Jean-Marc Sotiropoulos, Lawrence M. Henling, Michael W. Day, Jay A. Labinger, and John E. Bercaw
Chemical Science, **2013**, *4*, 2117-2121.

287. Frontiers, Opportunities, and Challenges in Biochemical and Chemical Catalysis of CO_2 Fixation
Aaron Appel, Andrew Bocarsly, John Bercaw, Holger Dobbek, Michel Dupuis, Daniel L., DuBois,* J. Gregory Ferry, Etsuko Fujita, Russ Hille, Paul J. A. Kenis, Cheryl A. Kerfeld, Robert Morris, Chuck Peden, Archie Portis, Steve Ragsdale,* Thomas B. Rauchfuss,* Joost N. H. Reek, Lance Seefeldt, Mark Spitler, Robert Stack, Rolf Thauer, Grover Waldrop
Chem. Rev., **2103**, *113*, 6621-6658.

288. Group 4 Transition-Metal Complexes of an Aniline-Carbene-Phenol Ligand
Emmanuelle Despagnet-Ayoub, Lawrence M. Henling, Jay A. Labinger, and John E. Bercaw
Organometallics, **2013**, *32*, 2934-2938.

289. Alkyne Hydroamination and Trimerization with Titanium *Bis*(phenolate)pyridine Complexes: Evidence for Low-Valent Titanium Intermediates and an Ethylene Adduct of Ti(II)
Ian A. Tonks, Josef C. Meier, and John E. Bercaw
Organometallics, **2013**, *32*, 3451-3457.

290. Trivalent Zirconocene Complexes – Investigation of Species Derived from *ansa*-Zirconocene-Based Olefin-Polymerization Catalysts by EPR- and NMR-Spectroscopy
Taylor N. Lenton, John E. Bercaw, Valentina N. Panchenko, Vladimir A. Zakharov, Dmitrii E. Babushkin, Igor E. Soshnikov, Evgenii P. Talsi, Hans H. Brintzinger
J. Am. Chem. Soc., **2013**, *135*, 10710-10719.

291. Kinetics and Mechanism of Indene C-H Bond Activation by $[(COD)Ir(\mu\text{-}OH)]_2$
Tonia S. Ahmed, Ian. A. Tonks, Jay A. Labinger, and John E. Bercaw
Organometallics, **2013**, *32*, 2934-2938.

293. Addition of a Phosphine Ligand Switches an *N*-Heterocyclic Carbene-Zirconium Catalysts from Oligomerization to Polymerization of 1-Hexene
Emmanuelle Despagnet-Ayoub, Lawrence M. Henling, Jay A. Labinger, and John E. Bercaw
Dalton Transactions, **2013**, *42*, 15544-15547.

299. Investigations into Asymmetric Post-Metallocene Group 4 Complexes for the Synthesis of Highly Regioirregular Polypropylene
Rachel C. Klet, Curt N. Theriault, Jerzy Klosin, Jay A. Labinger, and John E. Bercaw
Macromolecules, in press.

References to Technical Report`

[1]. For reviews on Ziegler-Natta polymerization see: (a) Brintzinger, H. H.; Fischer, D.; Mülhaupt, R.; Rieger, B.; Waymouth, R. M., Stereospecific olefin polymerization with chiral metallocene catalysts, *Angew. Chem. Intl. Ed. Engl.* **1995**, *34*, 1143.
(b) Gibson, V. C.; Spitzmesser, S. K., Advances in non-metallocene olefin polymerization catalysis. *Chem. Rev.*. **2003**, *103*, 283.
(c) Coates G. W. Precise control of polyolefin stereochemistry using single-site metal catalyst, *Chem. Rev.* **2000**, *100*, 1223.
(d) Resconi, L.; Cavallo, L.; Fait, A.; Piemontesi, F., Selectivity in propene polymerization with metallocene catalysts, *Chem. Rev.* **2000**, *100*, 1253.
(f) Domski, G. J.; Rose, J. M.; Coates, G. W.; Bolig, A. D.; Brookhart, M. Living alkene polymerization: new methods for the precision synthesis of polyolefins. *Prog. Polym. Sci.* **2007**, *32*, 30.

[2]. Matsugi, T.; Fujita, T. High performance olefin polymerization catalysts discovered on the basis of a new catalyst design concept. *Chem. Soc. Rev.* **2008**, *37*, 1264.

[3]. (a) Johnson, L. K.; Killian, C. M.; Brookhart, M., New Pd(II)-based and Ni(II)-based catalysts for polymerization of ethylene and α–olefins, *J. Am. Chem. Soc.* **1995**, *117*, 6414
(b) Johnson, L. K.; Mecking, S.; Brookhart, M., Copolymerization of ethylene and propylene with functionalized vinyl monomers by palladium(II) catalysts, *J. Am. Chem. Soc.* **1996**, *118*, 267.
(c) Ittel, S. D.; Johnson, L. K.; Brookhart, M., Late-metal catalysts for ethylene homo- and copolymerization, *Chem. Rev.* **2000**, *100*, 1169.
(d) Tempel, D.J.; Johnson, L.K.; Huff, R. L.; White, P. S.; Brookhart, M., Mechanistic studies of Pd(II)-alpha-diimine-catalyzed olefin polymerizations, *J. Am. Chem. Soc.* **2000**, *122*, 6686.
(e) Hicks, F. A., Brookhart, M., A highly active anilinotropone-based neutral nickel(II) catalyst for ethylene polymerization, *Organometallics* **2001**, *20*, 3217.
(f) Liu, W. J.; Malinoski, J. M.; Brookhart, M., Ethylene polymerization and ethylene/methyl 10-undecenoate copolymerization using nickel(II) and palladium(II) complexes derived from a bulky P,O chelating ligand, *Organometallics* **2002**, *21*, 2836.
(g) Daugulis O, Brookhart M., Polymerization of ethylene with cationic palladium and nickel catalysts containing bulky nonenolizable imine-phosphine ligands, *Organometallics* **2002**, *21*, 5926.
(h) Williams B. S., Leatherman M. D., White P.S., Brookhart, M., Reactions of vinyl acetate and vinyl trifluoroacetate with cationic diimine Pd(II) and Ni(II) alkyl complexes: Identification of problems connected with copolymerizations of these monomers with ethylene, *J. Am. Chem. Soc.* **2005**, *127*, 5132.

[4]. (a) Small, B. L.; Brookhart, M., Iron-based catalysts with exceptionally high activities and selectivities for oligomerization of ethylene to linear α-olefins, *J. Am. Chem. Soc.* **1998**, *120*, 7143.
(b) Britovsek, G. J. P.; Gibson, V. C.; Kimberley, B. S.; Maddox, P. J.; McTavish, S. J.; Solan, G. A.; White, A. J. P.; Williams, D. J., Novel olefin polymerization catalysts based on iron and cobalt, *Chem. Commun.* **1998**, 849.
(c) LePichon, L.; Stephan, D. W.; Gao, X. L.; Wang, Q. Y., Iron phosphinimide and phosphinimine complexes: Catalyst precursors for ethylene polymerization, *Organometallics*, **2002**, *21*, 1362.

[5]. (a) Canich, J. M. Eur. Patent 420 436, 1991.
(b) Canich, J. M.; Hlatky, G. G.; Turner, H. W. U. S. Patent 542 236, 1990.
(c) Stevens, J. C.; Timmers, F. J.; Wilson, D. R.; Schmidt, G. F.; Nickias, P. N.; Rosen, R. K.; Knight, G. W.; Lai, S. Eur. Patent 416 815, 1990.
(d) Arriola, D. J.; Carnahan, E. M.; Hustad, P. D.; Kuhlman, R. L.; Wenzel, T.T. *Science* 5 May, **2006** 714.
(e) Matsugi, T.; Fujita, T. High performance olefin polymerization catalysts discovered on the basis of a new design concept, *Chem. Soc. Rev.* **2008**, *37*, 1264.

[6]. (a) Takahashi, T., Hasegawa, M., Sukuzi, N., Saburi, M., Rousset, C.J., Fanwick, P.E., Negishi, E. Zirconium-catalyzed highly regioselective hydrosilation reaction of alkenes and x-ray structures of silyl(hydrido)zirconocene derivatives, *J. Am. Chem. Soc.*, **1991**, *113*, 8564.
(b) Eisch, J.J., Rhee, S-G., Kinetic, Stereochemical, and Molecular Association Factors in the Hydroalumination

of Alkynes. An Inquiry into the Intermediacy of π Complexes, *J. Am. Chem. Soc.*, **1974**, *96*, 7276.
(c) Beletskaya, I., Pelter, A., Hydroborations Catalyzed by Transition Metal Complexes, *Tetrahedron*, **1997**, *53*, 4957.
(d) Petros, R. A., Camara, J.M., Norton, J.R., Enantioselective Methylalumination of α-olefins, *J. Organomet. Chem.*, **2007**, *692*, 4768.
(e) Bytschkov, I., Doye, S., Group IV Metal Complexes as Hydroamination Catalysts, *Eur. J. Org. Chem.*, **2003**, 935.

[7]. Soulivong, D., Norsic, S., Taoufik, M., Coperet, C., Thivolle-Cazat, J., Chakka, S., Basset, J.M., Non-Oxidative Coupling Reaction of Methane to Ethane and Hydrogen Catalyzed by the Silica-Supported Tantalum Hydride: (-SiO)2 Ta-H. *J. Am. Chem. Soc.*, **2008**, *130*, 5044.

[8]. (a) Andes, C., Harkins, S.B., Murtuza, S., Oyler, K., Sen, A., New Tantalum Based Catalyst System for the Selective Trimerization of Ethene to 1-Hexene, *J. Am. Chem. Soc.*, **2001**, *123*, 7423.
(b) Deckers, P.J.W.; Hessen, B.; Teuben, J.H. Catalytic trimerization of ethene with highly active cyclopentadienyl-arene titanium catalysts **2002**, *Organometallics, 21*, 5122.
(c) Albahily, K.; Koc, E.; Al-Balawi, D.; Savard, D.; Gambarotta, S.; Burchell, T. J.; Duchateau, R., Chromium catalysts supported by a nonspectator NPN ligand: Isolation of single-component chromium polymerization catalysts, *Angew. Chem., Int. Ed. Engl.* **2008**, *47*, 5816.

[9]. (a) Goldman, A.S., Roy, A.H., Huang, Z., Ahuja, R., Schinski, W., Brookhart, M., Catalytic Alkane Metathesis by Tandem Alkane Dehydrogenation-Olefin Metathesis, Science, **2006**, *312*, 257.
(b) Bailey, B.C., Schrock, R.R., Kundu, S., Goldman, A.S., Huang, Z., Brookhart, M. Evaluation of Molybdenum and Tungsten Metathesis Catalysts for Homogeneous Tandem Alkane Metathesis, Organometallics, **2009**, *28*, 355.
(c) Basset, J.M.; Coperet, C.; Soulivong, D.; Taoufik, M.; Thivolle-Cazat, J., From olefin to alkane metathesis: A historical point of view, *Angew. Chem., Int. Ed. Engl.* **2006**, *45*, 6082.

[10]. (a) Piers, W. E.; Bercaw, J. E., α-Agostic assistance in Ziegler-Natta polymerization of olefins – Deuterium isotopic perturbation of stereochemistry indicating coordination of an α-C-H bond in chain propagation, *J. Amer. Chem. Soc.* **1990**, *112*, 9406.
(b) Krauledat, H.; Brintzinger, H. H., Isotope effects associated with α-olefin insertion in zirconocene-based poymerization catalysts – Evidence for an α-agostic transition state, *Angew. Chem. Int. Ed. Engl.* **1990**, *102*, 1412.
(c) Leclerc, M. K.; Brintzinger, H. H., Ansa-metallocene derivatives 31. Origins of stereoselectivity and stereoerror formation in ansa-zirconocene-catalyzed isotactic propene polymerization – A deuterium labeling study, *J. Am. Chem. Soc.* **1995**, *117*, 1651.
(d) Grubbs, R. H.; Coates, G. W., α-Agostic interactions and olefin insertion in metallocene polymerization catalysts, *Acc. Chem. Res.* **1996**, *29*, 85.
(e) Chirik, P.J.; Dalleska, N.F.; Henling,L. M.; Bercaw, J. E., Experimental evidence for γ-agostic assistance in β-methyl elimination, the microscopic reverse of α-agostic assistance in the chain propagation step of olefin polymerization, *Organometallics* **2005**, *24*, 2789.

[11]. Mitchell, J. P.; Hajela, S.; Brookhart, S. K.; Hardcastle, K. I.; Henling, L. M.; Bercaw, J. E., Preparation and structural characterization of an enantiomerically pure, C_2-symmetric, single-component Ziegler-Natta α-olefin polymerization catalyst, *J. Am. Chem. Soc.* **1996**, *118*, 1045.

[12]. Gilchrist, J. H.; Bercaw, J. E., New NMR spectroscopic probe of the absolute stereoselectivity for metal-hydride and metal-alkyl additions to the carbon-carbon double bond. Demonstration with a single-component, isospecific Ziegler-Natta α-olefin polymerization catalyst, *J. Am. Chem. Soc.* **1996**, *118*, 12021.

[13]. (a) Corradini, P.; Guerra, G.; Vacatello, M.; Villani, V., A possible model for site control of stereoregularity in the isotactic specific homogeneous Ziegler-Natta polymerization, *Gazz. Chim. Ital.* **1988**, *118*, 173.
(b) Corradini, P.; Busico, V.; Cavallo, L. Guerra, G.; Vacatello, M.; Venditto, V., Structural analogies between homogeneous and heterogeneous catalysts for the stereospecific polymerization of 1-alkenes, *J. Mol. Catal.* **1992**, *74*. 433.

(d) Guerra, G.; Corradini, P.; Cavallo, L.; Vacatello, M., Molecular mechanics and mechanisms of regulation of the stereospecificity in Ziegler-Natta catalysis, *Makromol. Chem., Makromol. Symp.* **1995**, *89*, 307.

[14]. (a) Leclerc, M. K.; Brintzinger, H.-H., Zr-Alkyl isomerization in ansa-zirconocene-catalyzed olefin polymerizations. Contributions to stereoerror formation and chain termination, *J. Am. Chem. Soc.* **1996**, *118*, 9024.
(b) Longo, P.; Grassi, A.; Pellecchia, C.; Zambelli, A., C-13 enriched end groups of isotactic polypropylene and poly(1-butene) prepared in the presence of ethylenediindenyldimethyltitanium and methyl alumoxane, *Macromolecules* **1987**, *20*, 1015.
(c) Zambelli, A.; Pellecchia C. *Makromol. Chem. Mackromol. Symp.* **1993**, *66*, 1.

[15]. Herzog, T. A.; Zubris, D. L.; Bercaw, J. E., A new class of zirconocene catalysts for the syndiospecific polymerization of propylene and its modification for varying polypropylene from isotactic to syndiotactic, *J. Am. Chem. Soc.* **1996**, *118*, 11988.

[16]. Veghini, D.; Henling, L. M.; Burkhardt, T. J.; Bercaw, J. E., Mechanisms of stereocontrol for doubly silylene-bridged C_s and C_1-symmetric zirconocene catalysts for propylene polymerization. Synthesis and molecular structure of $Li_2[(1,2\text{-}Me_2Si)_2\{C_5H_2\text{-}4\text{-}(1R,2S,5R\text{-menthyl})\}\{C_5H\text{-}3,5\text{-}(CHMe_2)_2\}].3THF$ and $[(1,2\text{-}Me_2Si)_2\{\eta^5\text{-}C_5H_2\text{-}4\text{-}(1R,2S,5R\text{-menthyl})\}\{\eta^5\text{-}C_5H\text{-}3,5\text{-}(CHMe_2)_2\}]ZrCl_2$, *J. Am. Chem. Soc.* **1999**, *121*, 564.

[17]. Yoder, J. C.; Day, M. W.; Bercaw, J. E., Racemic-meso interconversion for ansa-scandocene and ansa-yttrocene derivatives. Molecular structures of *rac*-$\{Me_2Si[\eta^5\text{-}C_5H_2\text{-}2,4\text{-}(CHMe_2)_2]_2\}ScCl \cdot LiCl(THF)_2$, $[$*meso*-$\{Me_2Si[\eta^5\text{-}C_5H_2\text{-}2,4\text{-}(CHMe_2)_2]_2\}Y(\mu\text{-}Cl_2)]_2$, and *meso*-$\{Me_2Si[\eta^5\text{-}C_5H_2\text{-}2,4\text{-}(CHMe_2)_2]_2\}Zr(NMe_2)_2$, *Organometallics* **1998**, *17*, 4946.

[18]. Miyake, S.; Henling, L. M.; Bercaw, J. E., Synthesis, molecular structure, and racemate-meso interconversion for *rac*-$(Me_2Si)_2\{\eta^5\text{-}C_5H\text{-}3\text{-}(CHMe_2)\text{-}5\text{-}Me\}_2MCl_2$ (M = Ti and Zr), *Organometallics* **1998**, *17*, 5528.

[19]. Abrams, M. B.; Yoder, J. C.; Loeber, C.; Day, M. W.; Bercaw, J. E., Fluxional η^3-allyl derivatives of ansa-scandocenes and an ansa-yttrocene. Measurements of the barriers for the η^3- to η^1- process as an indicator of olefin binding energy to d^0 metallocenes, *Organometallics*, **1999**, *18*, 1389.

[20]. Chirik, P. J.; Day, M. W. Day; Bercaw, J. E., Preparation and characterization of monomeric and dimeric group IV metallocene dihydrides having alkyl-substituted cyclopentadienyl ligands, *Organometallics* **1999**, 18 1873.

[21]. Chirik, P. J.; Day, M. W.; Labinger, J. A.; Bercaw, J. E., Alkyl rearrangement processes in organozirconium complexes. Observation of internal alkyl complexes during hydrozirconation, *J. Am. Chem. Soc.* **1999**, *121*, 10308.

[22]. Chirik, P. J.; Henling, L. M.; Bercaw, J. E., Synthesis of singly and doubly bridged ansa-zirconocene hydrides. Formation of an unusual mixed valence trimeric hydride by reaction of H_2 with $\{(Me_2Si)_2(\eta^5\text{-}C_5H_3)_2\}Zr(CH_3)_2$ and generation of a dinitrogen complex by reaction of N_2 with a zirconocene dihydride, *Organometallics* **2001**, *20*, 534.

[23]. Miller, S. A.; Bercaw, J. E., Aminofluorenyl-pentamethylcyclopentadienyl and bis(aminofluorenyl) derivatives of group 4 metals, *Organometallics* **2000**, *19*, 5608.

[24]. Wendt, O. F.; Bercaw, J. E., Thermally stable dialkylzirconocenes with β-hydrogens. Synthesis and diastereoselectivity, *Organometallics* **2001**, *20*, 3891.

[25]. Chirik, P. J.; Zubris, D. L.; Ackerman, L. J.; Henling, L. M.; Day, M. W.; Bercaw, J. E., Preparation of ansa-niobocene and ansa-tantalocene olefin hydride complexes as transition state analogues in metallocene-catalyzed olefin polymerization, *Organometallics* **2003**, *22*, 172.

[26]. Ackerman, L. J.; Green, M. L. H.; Green, J. C.; Bercaw, J. E., Experimental and theoretical studies of olefin insertion for ansa-niobocene and ansa-tantalocene ethylene hydride complexes, *Organometallics* **2003**, *22*, 188.

[27]. Miller, S. A.; Bercaw, J. E., Isotactic-hemiisotactic polypropylene from C_s-symmetric ansa-metallocene catalysts: A new strategy for the synthesis of elastomeric polypropylene, *Organometallics* **2002**, *21*, 934.

[28]. US Patent No. 6,469,188 B1; issued October 22, 2002.

[29]. Brandow, C.; Mendiratta, A.; Bercaw, J. E., Ancillary ligand and olefin substituent effects on olefin dissociation for cationic zirconocene complexes bearing a coordinated pendant olefin, *Organometallics* **2001**, *20*, 4253.

[30]. Busico, V.; Cipullo, R., Influence of monomer concentration on the stereospecificity of 1-alkene polymerization promoted by C_2-symmetric ansa-metallocene catalysts, *J. Am. Chem. Soc.* **1994**, *116*, 9329.

[31]. Resconi, L., On the mechanisms of growing-chain-end isomerization and transfer reactions in propylene polymerization with isospecific, C_2-symmetric zirconocene catalysts, *J. Mol. Catal. A: Chem* **1999**, *146*, 167.

[32]. Miller, S. A.; Bercaw, J. E., Highly Stereoregular Syndiotactic Polypropylene Formation with Metallocene Catalysts via Influence of Distal Ligand Substituents, *Organometallics* **2004**, *23*, 1777.

[33]. Chrik, P. J.; Bercaw, J. E., Cyclopentadienyl and olefin substituent effects on insertion and β-hydrogen elimination with group 4 metallocenes. Kinetics, mechanism and thermodynamics for zirconocene and hafnocene alkyl hydride derivatives, *Organometallic*s **2005**, *24*, 5407.

[34]. Elowe, P. R.; McCann, C.; Pringle, P. G.; Spitzmesser, S. K. and Bercaw, J. E., Nitrogen-Linked Diphosphine Ligands with Ethers Attached to Nitrogen for Chromium Catalyzed Ethylene Tri- and Tetramerizations, *Organometallics*, **2006**, *25*, 5255-5260.

[35]. Agapie, T.; Labinger, J. A.; Bercaw, J. E., Mechanistic Studies of Olefin and Alkyne Trimerization with Chromium Catalysts – Deuterium Labeling and Studies of Regiochemistry Using a Model Chromacyclopentane Complex, *J. Am. Chem. Soc.* **2007**, *129*, 14281.

[36]. Min, E.Y.; Byers, J. A.; Bercaw, J. E., Catalyst Site Epimerization during the Kinetic Resolution of Chrial α Olefins by Polymerization, *Organometallics* **2008**, *27*, 2179.

[37]. Byers, J. A.; Bercaw, J. E., Kinetic Resolution of Racemic α-Olefins with *Ansa* Zirconocene Polymerization Catalysts: Enantiomorphic Site vs. Chain End Control, *PNAS,* **2006**, *103* 15303.

[38]. Marinescu, S.; Agapie, T.; Day, M. W.; Bercaw, J. E., Group 3 Diakyl Complexes with Tetradentate (L, L, N, O; L = N, O, S) Monoanionic Ligands—Synthesis and Reactivity, *Organometallics,* **2007**, *26*, 1178.

[39] (a) Wolczanski, P. T., Chemistry of electrophilic metal centers coordinated by silox (t-Bu_3SiO), tritox (t-Bu_3CO) and related bifunctional ligands, *Polyhedron* **1995**, *14*, 3335.
(b) Coates, G. W.; Hustad, P. D.; Reinartz, S., Catalysts for the living insertion polymerization of alkenes: Access to new polyolefin architectures using Ziegler-Natta chemistry, *Angew. Chem., Int. Ed. Engl.* **2002**, *41*, 2236.
(c) Watson, D. A.; Chiu, M.; Bergman, R. G., Zirconium bis(amido) catalysts for asymmetric intramolecular alkene hydroamination, *Organometallics* **2006**, *25*, 4731.
(d) Anderson, L. L.; Arnold, J.; Bergman, R. G., Proton-catalyzed hydroamination and hydroarylation reactions of anilines and alkenes: A dramatic effect of counteranions on reaction efficiency, *J. Am. Chem. Soc.* **2005**, *127*, 14542.
(e) Ackermann, L.; Bergman, R. G.; Loy, R. N., Use of group 4 bis(sulfonamido) complexes in the intramolecular hydroamination of alkynes and allenes, *J. Am. Chem. Soc.* **2003**, *125*, 11956.
(f) Rothwell, I. P., A new generation of homogeneous arene hydrogenation catalysts, *Chem. Commun.* **1997**, 1331.
(g) Wallace, K. C.; Liu, A. H.; Dewan, J. C.; Schrock, R. R., Preparation abd reactions of tantalum Alkylidene complexes containing buky phenoxide or thiolate ligands – controlling ring-opening metathesis polymerization activity and mechanism through choice of anionic ligand, *J. Am. Chem. Soc.* **1988**, *110*, 4964.
(h) Schrock, R. R.; Hoveyda, A. H., Molybdenum and tungsten imido alkylidene complexes as efficient olefin-metathesis catalysts, *Angew. Chem., Int. Ed. Engl.* **2003**, *42*, 4592.
(i) Tsang, W. C. P.; Hultzsch, K. C.; Alexander, J. B.; Bonitatebus, P. J.; Schrock, R. R.; Hoveyda, A. H., Alkylidene and metalacyclic complexes of tungsten that contain a chiral biphenoxide ligand. Synthesis, asymmetric ring-closing metathesis, and mechanistic investigations, *J. Am. Chem. Soc.* **2003**, *125*, 6337.
(j) Schrock, R. R., High oxidation state multiple metal-carbon bonds, *Chem. Rev.* **2002**, *102*, 145.
(k) Spencer, L. P.; Beddie, C.; Hall, M. B.; Fryzuk, M. D., Synthesis, reactivity, and DFT studies of tantalum

complexes incorporating diamido-N-heterocyclic carbene ligands. Facile endocyclic C-H bond activation, *J. Am. Chem. Soc*. **2006**, *128*, 12531.

[40]. Agapie, T.; Henling, L. H.; DiPasquale, A. G.; Rheingold, A.; Bercaw, J. E., Zirconium and Titanium Complexes Supported by Tridentate LX_2 Ligands having Two Phenolates Linked to Furan, Thiophene, and Pyridine Donors: Precatalysts for Propylene Polymerization and Oligomerization, *Organometallics* **2008**, *27*, 6245.

[41]. (a) Baumann, R.; Stumpf, R.; Davis, W. M.; Liang, L.-C.; Schrock, R. R., Titanium and zirconium complexes that contain the tridentate diamido ligands $[(i\text{-}PrN\text{-}o\text{-}C_6H_4)_2O]^{2-}$ ($[i\text{-}PrNON]^{2-}$) and $[(C_6H_{11}N\text{-}o\text{-}C_6H_4)_2O]^{2-}$ ($[CyNON]^{2-}$), *J. Am. Chem. Soc.* **1999**, *121*, 7822.
(b) Flores, M. A.; Manzoni, M. R.; Baumann, R.; Davis, W. M.; Schrock, R. R., Zirconium Complexes That Contain a Diamido O-Donor Ligand with a Restricted Geometry, *Organometallics* **1999**, *18*, 3220.
(c) Schrock, R. R.; Seidel, S. W.; Schrodi, Y.; Davis, W. M., Synthesis of Zirconium Complexes That Contain the Diamidophosphine Ligands $[(Me_3SiNCH_2CH_2)_2PPh]^{2-}$ or $[(RNSiMe_2CH_2)_2PPh]^{2-}$ (R = t-Bu or 2,6-$Me_2C_6H_3$), *Organometallics* **1999**, *18*, 428.
(d) Graf, D. D.; Schrock, R. R.; Davis, W. M.; Stumpf, R., Synthesis of Zirconium Complexes Containing the Tridentate Diamido Ligands $[(t\text{-}Bu\text{-}d_6\text{-}N\text{-}o\text{-}C_6H_4)_2S]^{2-}$ and $[(i\text{-}PrN\text{-}o\text{-}C_6H_4)_2S]^{2-}$, *Organometallics* **1999**, *18*, 843.
(e) Aizenberg, M.; Turculet, L.; Davis, W. M.; Schattenmann, F.; Schrock, R. R., Synthesis of Group 4 Complexes That Contain the Tridentate Diamido/Donor Ligands $[(ArylNCH_2CH_2)_2O]^{2-}$ and Zirconium Complexes That Contain $[(ArylNCH_2CH_2)_2S]^{2-}$ and an Evaluation of Their Activity for the Polymerization of 1-Hexene, *Organometallics* **1998**, *17*, 4795.

[42]. (a) Tshuva, E. Y.; Goldberg, I.; Kol, M.; Goldschmidt, Z., Zirconium complexes of amine-bis(phenolate) ligands as catalysts for 1-hexene polymerization: Peripheral structural parameters strongly affect reactivity, *Organometallics* **2001**; *20*, 3017.
(b) Tshuva, E. Y.; Goldberg, I.; Kol, M.; Weitman, H.; Goldschmidt, Z., Novel zirconium complexes of amine bis(phenolate) ligands. Remarkable reactivity in polymerization of hex-1-ene due to an extra donor arm, *Chem. Commun.* **2000**; 379.
(c) Tshuva, E. Y.; Groysman, S.; Goldberg, I.; Kol, M.; Goldschmidt, Z., [ONXO]-type amine bis(phenolate) zirconium and hafnium complexes as extremely active 1-hexene polymerization catalysts, *Organometallics* **2002**, *21*, 662.
(d) Groysman, S.; Goldberg, I.; Kol, M.; Genizi, E.; Goldschmidt, Z., Group IV complexes of an amine bis(phenolate) ligand featuring a THF sidearm donor: from highly active to living polymerization catalysts of 1-hexene, *Inorganica Chimica Acta* **2003**, *345*, 137.
(e). Tshuva, E. Y.; Goldberg, I.; Kol, M.; Goldschmidt, Z., Living polymerization and block copolymerization of alpha-olefins by an amine bis(phenolate) titanium catalyst, *Chem. Commun.* **2001**; 2120.

[43]. Agapie, T. A.; Day, M. W.; Bercaw, J. E., Synthesis and Reactivity of Tantalum Complexes Supported by Bidentate X_2 and Tridentate LX_2 Ligands having Two Phenolates Linked to Pyridine, Thiophene, Furan, and Benzene Connectors – Mechanistic Studies of the Formation of a Tantalum Benzylidene and Insertion Chemistry for Tantalum-Carbon Bonds, *Organometallics* **2008**, *27*, 6123.

[44]. Schrock, Richard R.; Messerle, Louis W.; Wood, Clayton D.; Guggenberger, Lloyd J. Multiple metal - carbon bonds. 9. Preparation and characterization of several alkylidene complexes, $M(\eta^5\text{-}C_5H_5)_2$(alkylidene)X (M = tantalum or niobium), and the x-ray structure of $Ta(\eta^5\text{-}C_5H_5)_2(CHC_6H_5)(CH_2C_6H_5)$. An investigation of alkylidene ligand rotation. *J. Am. Chem. Soc.* **1978**, *100*, 3793.

[45]. Theodor Agapie, T.; Bercaw, J. E., Cyclometallated Tantalum Diphenolate Pincer Complexes: Intramolecular C-H/M-CH_3 σ Bond Metathesis May be Faster than O-H/M-CH_3 Protonolysis, *Organometallics* **2007**, *26*, 2957.

[46]. Baldwin, S. M.; Bercaw, J. E.; Brintzinger, H-H., Alkylaluminum-Complexed Zirconocene Hydrides: Identification of Hydride-Bridged Species by NMR Spectroscopy, *J. Am. Chem. Soc.* **2008**, *130*, 17423.

[47]. Bulls, A. R.; Schaefer, W. P.; Serfas, M.; Bercaw, J. E., Intramolecular C-H bond activation of benzyl ligands by Metallated-Cyclopentadienyl Derivatives of Permethylhafnocene. Molecular Structure of

(η^5-C_5Me_5)(η^5,η^1-$C_5Me_4CH_2$)$HfCH_2C_6H_5$ and the mechanism of rearrangement to its hafnabenzocyclobutene tautomer (η^5-C_5Me_5)$_2$Hf(CH_2-*o*-C_6H_4), *Organometallics* **1987,** *6*, 1219.

[48]. Tonks, I. A.; Larry M. Henling, L. M.; Michael W. Day, M. W.; Bercaw, J. E., Amine, amido, and imido complexes of tantalum supported by a pyridine-linked bis(phenolate) pincer ligand. Ta-N π bonding influences pincer ligand geometry, *Inorg. Chem.*, ASAP.

[49]. Parkin, G.; van Asselt, A.; Leahy, D. J.; Whinnery, L.; Hua, N. G.; Quan, R. W.; Henling, L. M.; Schaefer, W. P.; Santarsiero, B. D.; Bercaw, J. E., Oxo-Hydrido and oxo-imido derivatives of permethyltantalocene- structures of (η^5-C_5Me_5)$_2$Ta(=O)H and (η^5-C_5Me_5)$_2$Ta(=NPh)H- doubly or triply bonded tantalum ox and imido ligands, *Inorg. Chem.* **1992**, *31*, 82.

[50]. Weintrob, E. C.; Tofan, D.; Bercaw, J. E. Synthesis and characterization of iron derivatives having a pyridine-linked bis(anilide) pincer ligand. *Inorg. Chem.* **2009**, *48*, 3808.